Bachelor Project

Czech Technical University in Prague

F3

Faculty of Electrical Engineering
Department of Cybernetics

Decentralized Localization of Active RFID Transmitters by a Group of Unmanned Aerial Vehicles

Jakub Pogran

Supervisor: Ing. Martin Saska Dr. rer. nat.
Field of study: Cybernetics and Robotics
Subfield: Robotics
May 2017

Czech Technical University in Prague
Faculty of Electrical Engineering

Department of Cybernetics

BACHELOR PROJECT ASSIGNMENT

Student: Jakub P o g r a n

Study programme: Cybernetics and Robotics

Specialisation: Robotics

Title of Bachelor Project: Decentralized Localization of Active RFID Transmitters by a Group of Unmanned Aerial Vehicles

Guidelines:

The goal of the thesis is to design, implement in ROS (Robot Operating System), and experimentally verify in Gazebo simulator and in real experiments a decentralized online algorithm for localization of RFID transmitters by a group of unmanned aerial vehicles (UAV). The following tasks will be solved:

- To implement a model of a sensor for measuring a strength of signal of transmitters [2,3] into the robotic Gazebo simulator based on results of real experiments.
- To design a simple method for localization of a static transmitter using gradient of the signal intensity measured in different positions in the simulator (the UAV group flies towards an estimated position of the RFID).
- To test influence of the size of the formation on the precision and reliability of the position estimation in a case of noisy measurements.
- To implement and test a Kalman filter [1] for an estimation of position of a moving ARFID.
- To realize an offline experiment with the multi-UAV platform of the Multi-Robot Systems group [4] (the signal intensity will be measured and the position of RFIDs computed after the experiments).
- To prepare a decentralized online experiment (UAVs will move based on the currently measured intensity). This experiments will be realized based on the platform availability, which will be decided by thesis advisor.

Bibliography/Sources:

[1] T. M. Bielawa. Position Location of Remote Bluetooth Devices. Blacksburg, VA, USA. Master's thesis. Virginia Polytechnic Institute and State University, 2005.
[2] J. Rodas, T. M. Fernandez, D. I. Iglesia, C. J. Escudero. Multiple Antennas Bluetooth System for RSSI Stabilization, in Wireless Communication Systems, 2007.
[3] S. J. Julier and J. K. Uhlmann. A New Extension of the Kalman Filter to Nonlinear Systems. In Proc. of AeroSense: The 11th Int. Symp. On Aerospace/Defence Sensing, Simulation and Controls, 1997.
[4] T. Baca, G. Loianno and M. Saska. Embedded Model Predictive Control of Unmanned Micro Aerial Vehicles. In 21st International Conference on Methods and Models in Automation and Robotics (MMAR). 2016.

Bachelor Project Supervisor: Ing. Martin Saska, Dr. rer. nat.

Valid until: the end of the summer semester of academic year 2017/2018

L.S.

prof. Dr. Ing. Jan Kybic
Head of Department

prof. Ing. Pavel Ripka, CSc.
Dean

Prague, February 14, 2017

Acknowledgements

I want to thank all people around me, specially to dr. Martin Saska for supervising me through this thesis. Further, I would like to thank to all people from MRS laboratory, especially Matouš Vrba, Tomáš Báča and Vojtěch Spurný for their help with the ROS and experiments. Furthermore I would like to thank all people who helped me with the text correction. Finally I want to thank my family.

Declaration

I declare that the presented work was developed independently and that I have listed all sources of information used within it in accordance with the methodical instructions for observing the ethical principles in the preparation of university theses.

Prague, 15. May 2017

Abstract

The need for accurate localization nowadays is growing more and more and it is concerning localization of both moving and static objects, things, animals, etc. Finding the location is often needed in order to search or monitor the targets, or conduct environmental mapping. The method of online decentralized localization of radio-frequency device using organized formation of unmanned autonomous helicopters is developed in this work. The algorithms that are used for localization are two: triangulation and Unscented Kalman filter. Both of the algorithms use the information about the distance between the searched transmitter and the receiver, which is attached to the unmanned helicopter, and this distance is determined by a predetermined pattern of radio signal propagation. Another topic that this thesis examines is the relative position, size, rotation, and distance of the formation from the localized object and how these parameters influence the accuracy of localization. The findings are taken into account when refining the estimated location during localization. In addition, an experimental platform has been developed which has enabled the work with real HW, and an experiment with a formation of drones has been carried out.

Keywords: unmanned aerial vehicle, localization, formation, triangulation, Unscented Kalman filter, radio-frequency identifier

Supervisor: Ing. Martin Saska Dr. rer. nat.

Abstrakt

Potřeba přesné lokalizace v současnosti stále více roste a to jak pohyblivých, tak statických objektů, věcí, zvířat, atd. Zjistit polohu je často potřeba z důvodu vyhledávání resp. sledování cílů, nebo mapování prostředí.V této práci je rozvedena metoda online decentralizovaného způsobu lokalizace radio-frekvenčního zdroje za pomoci organizované formace autonomních bezpilotních helikoptér. Algoritmy, které jsou použité k lokalizaci, jsou dva: triangulace a Unscented Kalman filter. Oba využívají znalost vzdálenosti hledaného vysílače od přijímače, který je připevněn na bezpilotní helikoptéře, a tato vzdálenost je určena pomocí předem daného modelu šíření rádiového signálu. Další problematikou, kterou se tato práce zabývá, je relativní pozice, velikost, rotace, a vzdálenost formace od lokalizovaného objektu a jak tyto parametry ovlivňují přesnost lokalizace. Tato zjištění jsou následně zohledněna při zpřesňování odhadované polohy během lokalizace. Dále byla vyvinuta experimentální platforma, díky které bylo možné pracovat s reálným HW, a nakonec proběhl i experiment s formací dronů.

Klíčová slova: UAV, lokalizace, formace, triangulace, Unscented Kalman filter, rádio-frekvenční identifikátor

Překlad názvu: Decentralizovaná lokalizace aktivních RFID čipů skupinou bezpilotních helikoptér

Contents

Figures

Chapter 1

Introduction

Many industries, such as agriculture, transport, heavy industry and others, are going through a phase of automation in the last years. Alongside with this, the need for accurate localization is increasing. One of the most extensive localization systems is GPS. Among the disadvantages of this system is the need to have a GPS locator that is very energy-intensive and inaccurate sometimes in the order of dozens of meters. Furthermore, GPS signal is not available everywhere.

A concept of localization radio frequency sources by a formation of unmanned aerial vehicles (UAV) is introduced in this work. UAVs are taken as a widely growing platform. They offer an advantage to explore territories even with hardly penetrable surfaces, such as meadows, flatted areas, fields, mountains, and more, in other words places where it is difficult to get by terrestrial robots. Drones are aerial vehicles which can fly without remote control. Therefore, they have a great potential to be used in areas without direct contact, for example, they could be used for fast search of people lost in avalanches, herd monitoring, or tracking other ground robots.

Another already widely explored area, this work looks into, is the use of more collaborative robots at the same time. On one hand, the robot collaboration gives a possibility to localize moving objects, for example animals, people, or even other robots, without collisions. On the other hand, a supervised system [LL08], [WYB07] that controls all robots is needed.

This thesis is build on a previous work at the Department of Cybernetics, at Czech Technical University in Prague. In a thesis [Vrb16] an approach is examined that is using Bluetooth devices and Extended Kalman filter to estimate searched position. The localizing of the transmitter of the signal is evaluated from the data previously obtained. However, used Bluetooth dongles have range only about 4 meters long. Which is not enough for outdoor localization system.

An online system that search and localize radio frequency beacon in the

specified area with a formation of the UAVs is introduced in this thesis.

1.1 State of the Art

The localization of a radio frequency (RF) device is a widespread topic. The frequent assumption is that the unit is on the ground, this premise reduces degrees of freedom into 2D space, therefore, complexity of the localization problem is reduced as well.

Two RS-based (received signal) techniques are the most commonly used for the localization of RF devices, namely, they are the fingerprinting and the propagation-based techniques. Both are based on measuring the received signal, however, with different use.

The fingerprinting techniques presented in [BP00], [PLM02], [Kae06] are composed of two phases, learning and localization. In the learning phase, data are measured and stored. After that, localization phase responds with finding the nearest neighbour in signal position space. This approach is mostly used for indoor localization with solid, stable and preinstalled infrastructure, for example, it is the standard wireless LAN used in [PLM02]. In an environment where there are lots of barriers and signal reflections, this approach offers a very fast and precise localization. On the other side, saved data must be recalibrated with every environmental change. The goal of this work is to be able to localize objects in areas with no infrastructure, or where previous measurements are not available, therefore, fingerprinting techniques are not fitting these requirements.

The propagation-based techniques, for example [CK02], [CDB05], [CHC06], are based on measuring ToA (time of arrival), AoA (angle of arrival), TDoA (time difference of arrival) or SS (signal strength). TDoA, ToA based algorithm [CHC06] needs calibration and time synchronization between base stations, or special devices to measure angle. SS based algorithms which account distance from signal strength can be used if there is a known model of signal propagation [FGP+10].

With an information about distances and multiple positions, triangulation based algorithms [PY05], [FGP+10] can be used. They offer a very fast and analytical way to estimate position. The disadvantage is a massive localization inaccuracy that can be caused by the environment interfering with the signal or signal reflection.

A different way of localization to triangulation based algorithms is the Kalman filtering based one [Mar08], [KCK06] which offers prediction and estimation of the states of the system. This filter can be also used to estimate the position of a moving target. For nonlinear systems, such as the one described in this paper, two types of Kalman filters are used, Extended and

Unscented Kalman filters. Extended filter [Vrb16] is older and broadly known, but as it is shown in [KCK06] it offers poor estimation for systems with high nonlinearity. That is caused by using Taylor series expansion as a linearization of the nonlinear functions. The second, a newer filter, is Unscented Kalman filter [WVDM00]. It uses propagation of sigma points through unscented transformation. When comparing the two filter types, the Unscented filter has a better performance at the expense of a higher computational time, but for the needs of this work it is not an obstacle.

Mobile robot platform is needed to search and localize in spacious areas, like fields or mountains. Multiple UAVs are used as a very versatile robot platform [PDTY09], [PY05], [GLBA15]. In the article [GLBA15] it is described that if transmitters are static, only one UAV can be utilized, and its measurements from the different positions can be combined to find the estimation. In [PDTY09] authors used more UAVs for a faster scan of a searching area with a non-formation method.

Flying in a formation (see [SBT+16], [SVKP14], [SKV+14], [SBS16], [SKP14] for theoretical work on formation flying) and self-stabilization is used in this work to ensure robustness and stability. There are many ways how to achieve this, some of the ways are trajectory planning, relatively vision stabilization, or global coordination system stabilization. In this work the differential GPS is used to localize and stabilize all UAVs. Moreover, each UAV has a fixed position in a formation, which is described in a Chapter 3. Collision avoidance is set up in advance to prevent unexpected behaviour.

1.2 Problem statement

The purpose of this work is to develop an online decentralized localization system using the mobile formation of UAVs and test it in real experiments. Used three UAVs are part of the "mbzirc" system developed by Multi-robot systems group of CTU in Prague. Each of the helicopter is localized by GPS location. Moreover, it has fully developed control system that offers 'Go To Position' command, and collision avoidance. All drones broadcast sensors data and communicate via wireless network. It is assumed that used radio frequency antenna has possibility to measure Received Signal Strength Indication (RSSI).

Simulations need to be conducted to verify algorithms. Therefore, model of an RSSI sensor based on results from real measurements has to be implemented. Another object of this work is to test how relative position formation influences the precision of estimated position in a case of noisy measurements.

Chapter 2

System Description

The system, is defined at the beginning in this chapter. Signal strength model with its parameters is examined in section 2.2, following by state-space model of the system formulated in section 2.3, which is used for estimation by Kalman filter. In section 2.4 it is defined how the transmitter and the receiving signal are simulated.

2.1 System Setup

It is said in the Chapter 1 that a group of unmanned aerial vehicles is used. Each of the UAVs is the same hexacopter with receiving antenna on it. A UAV control unit is a pixhawk 4 (For more information see [1]), which is open-hardware autopilot system. How UAVs are organized is written in Chapter 3. All robots run on Robotic Operating System, which ensures communication via wireless network between them. ROS is a collection of tools, libraries, and conventions that helps to develop robotic system across different robot platforms. More about ROS can be seen in [QCG+09].

Used technology to transmit and receive signal between beacon and the formation is radio 2.4GHz frequency units specifically a Digi XBeePRO S2B, ZigBee, which can be seen in Figure 2.1.

[1] `https://pixhawk.org/`

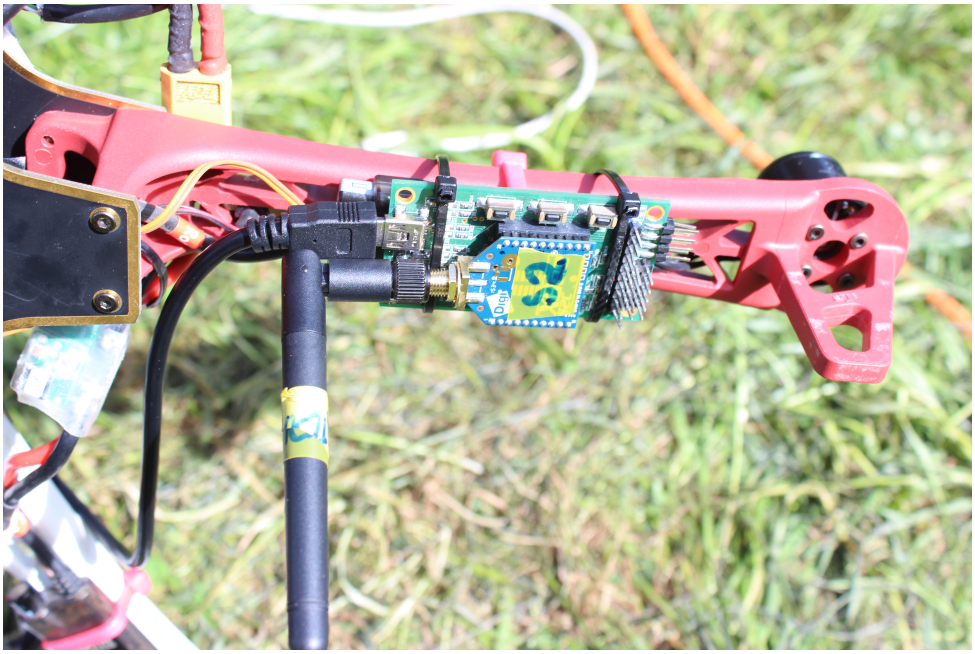

Figure 2.1: Photo of the XBee device with 2.4GHz antenna mounted onboard of the UAV.

It is assumed that beacon lies on the ground at zero altitudes.

All simulations in this work are made in a robotic simulator *Gazebo*. This simulator has an integrated ROS thanks to that the same code can be run by the simulator the same as by the real HW. The Gazebo can simulate group of helicopters with all of the on-board sensors and realistic behaviour and transmitting antenna in a given environment.

This work aims for development of a system for robust outdoor localization. Propagation of the signal is very sensitive to the obstacles in the environment and reflation. Therefore, an outdoor environment without any obstacles and interference, which could affect the distribution of the signal, is expected in all tests, experiments, and simulations. Green field with the flat ground is set as the standard environment. Experiments are conducted on a rectangular meadow with a size of 70×150 square meters.

2.2 Signal Strength

The information about distance between transmitter and receiver is needed for algorithms used. This section describes how this distance is calculated from Received Signal Strength Indication (RSSI).

Friis transmission equation (2.1) describes the strength of the receiving signal according to a distance between transmitting and receiving antennas

under ideal conditions. If the gain of transmitting and receiving signal have units in decibels, the equation can be formulated as

$$P_r = P_t + G_t + G_r + 20\log_{10}\left(\frac{\lambda}{4\pi R}\right), \tag{2.1}$$

where P_r is receiving power in decibel-milliwatts [dBm], P_t is transmitting power also in [dBm], G_t, G_r is transmitting and receiving antenna gain respectively, both in [dB]. λ is wavelength in [m] which can be obtained from the radio frequency and R is the distance between antennas also in [m].

This equation 2.1 has a condition that $R >> \lambda$. XBee with radio frequency 2.4 GHz is used for the real measurements. So wavelength is

$$\lambda = \frac{c}{f} = \frac{3 \times 10^8}{2.4 \times 10^9} = 0.125\ [m],$$

where c is speed of light in [m/s] and f is radio frequency of signal in [Hz]. So this model of signal strength can not be used in cases of small distances between transmitting and receiving antennas. The model is used for distances corresponding to meters. Therefore, this condition is not a problem and model of the signal strength can be used. More about distances at which model is used can be seen in section 2.2.1.

The equation (2.1) is not optimal and robust enough to model real signal strength. Moreover, this formula does not allow for noise deviation which can be caused by signal reflection, or by other radio sources. Model in lognormal form is used to cope with above-mentioned problems, which can be formulated as

$$P_r = P_0 - 10n\log_{10}(R) + \chi, \tag{2.2}$$

where P_r is receiving power in [dBm], R is distance between transmitting and receiving antennas in [m], P_0 and n are parameters, and χ is normal distributed noise. Parameters P_0 and n can be experimentally identified, which is in section 2.2.1. It is expected that the noise has a normal distribution and can be described as

$$\chi \sim \mathcal{N}(\mu_\chi,\ \sigma_\chi^2),$$

where μ is mean, and σ^2 is variance. Their values are specified in section 2.2.2.

2.2.1 Identification Parameters of Signal Strength Model

The two parameters that need to be determined are in equation (2.2). For parameter n it is assumed that $n = 2$ which is a parameter that corresponds to theoretical Friis curve. This assumption is confirmed by measurement. And the second parameter is obtained by fitting real measured data, which

can be seen in Figure 2.2. Parameter P_0 does not deform the curve; it only shifts the theoretical curve in y direction. So it is assumed that the curve corresponds to the Friis curve, so "fitting" data means to find P_0 that shifts theoretical curve in the position where error mean is zero, which is further described in section 2.2.2.

The experiment realized to measure RSSI characteristic, consists of two XBee modules, one used as transmitting antenna, which is located on the ground, and the 'receiver' which is attached on the UAV. Measured RSSI samples over distance can be seen in Figure 2.2. A position of the receiving antenna is known for each measurement using on-board GPS module. Position of transmitting and receiving antennas is known, therefore, Euclidean distance between transmitter and receiver is calculated.

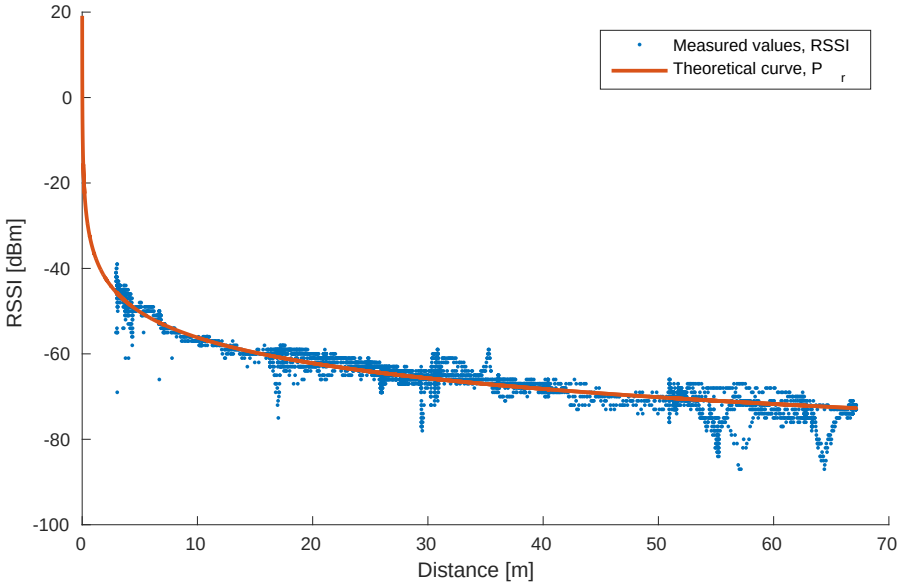

Figure 2.2: Measured RSSI samples depending on a distance. And fitted theoretical curve.

Above 6000 samples are measured throughout whole area from 4 meters up to 68 meters in between transmitter and receiver. Parameter of the fitted theoretical curve (equation (2.2)) is identified as $P_0 = -36$dBm.

No samples within 4 meters were taken, because the RSSI up to 4 meters is constant and equals to -31dBm thus there is no useful information about distance. In this area (closer than 4 meters from transmitter to receiver) algorithms can not localize transmitter. Therefore, the biggest usable sample (which algorithms use) corresponds to -32dBm. That means that active area (the area, where this model can be used), is between 4 and 70 meters from the transmitter to the receiver. At bigger distances communication between

XBee devices can not be ensured.

2.2.2 Noise

To model a signal strength that corresponds to real measurements, fitted curve is not enough. As can be seen in Figure 2.2, measured data do not correspond to theoretical values exactly; there is some noise. The error can be accounted to a difference between a measured sample and theoretical value corresponding to the same distance. This error can be seen in the Figure 2.3.

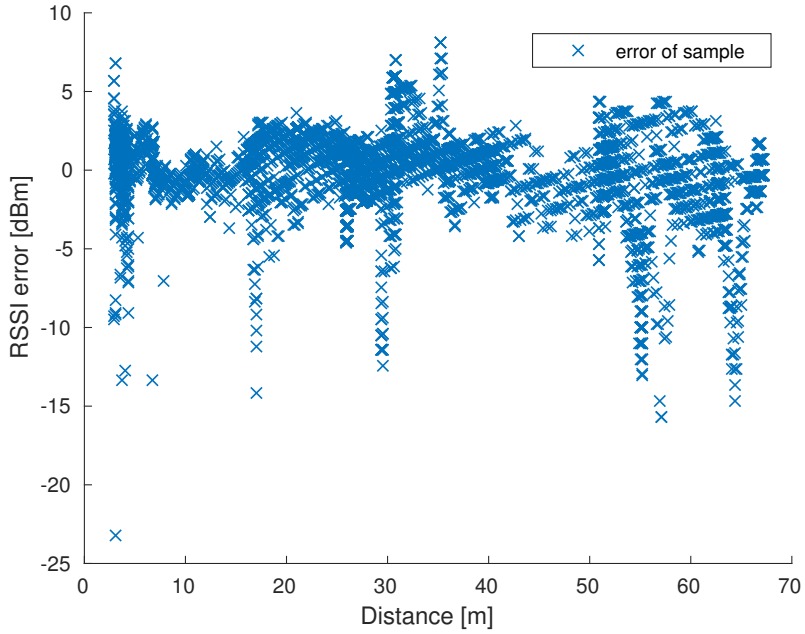

Figure 2.3: Difference between measured and theoretical value.

The error for every sample is calculated as

$$e_i = s_i - v_{theoretical}(d_i),$$

where s_i is the i-th sample, d_i is distance of the i-th sample, and $v_{theoretcal}(d_i)$ is value of the theoretical curve for distance of the i-th sample. As mentioned before in section 2.2.1, the theoretical curve is fitted in such a way that mean of error equals to zero. So the important parameter to model real signal is a standard deviation of this distribution, which is determined as

$$\sigma = \sqrt{\frac{1}{N-1}\sum_{i=1}^{N} e_i^2},$$

where N is number of samples and e_i is the i-th error. Standard deviation equals to $\sigma = 2.57$.

Therefore, it is assumed in the simulation that the noise of error χ corresponds to normal distribution with parameters as

$$\chi \sim \mathcal{N}(0,\ 2.57). \tag{2.3}$$

2.3 State-Space Representation of the System

Algorithm based on Unscented Kalman Filter is used to estimate the position of the moving transmitter, which is described in section 4.3. Discrete state-space representation of the system is needed, and can be described as

$$\vec{x}_k = \mathbf{A}\vec{x}_{k-1} + \mathbf{B}\vec{u}_k + \vec{w}_k, \tag{2.4}$$
$$\vec{y}_k = h(\vec{x}_k) + \vec{v}_k, \tag{2.5}$$

where $\vec{x}_k$ is the state vector at time k, $\mathbf{A}$ is the state matrix, $\mathbf{B}$ is the input matrix, $\vec{u}_k$ is the input vector, $\vec{y}_k$ is the measurement vector, and $h(\vec{x})$ is the non-linear function which maps the true state space in the observed space. $\vec{w}_k$ and $\vec{v}_k$ are the process noise and measurement noise, which are assumed to be with zero mean as

$$\vec{w}_k \sim \mathcal{N}(0,\ \mathbf{Q}_k),$$
$$\vec{v}_k \sim \mathcal{N}(0,\ \mathbf{R}_k),$$

where $\mathbf{Q}_k$ is the process noise covariance matrix and $\mathbf{R}_k$ is the measurement noise covariance matrix, described in section 4.3.

Matrices $\mathbf{A},\ \mathbf{B}$ are

$$\mathbf{A} = \mathbf{I}_{12\times 12},$$
$$\mathbf{B} = \mathbf{I}_{12\times 12}.$$

States are determined as coordinates of UAVs and beacon, respectively. The coordinates of UAVs and RSSI are set as measurements, and change of positions of the UAVs and beacon respectively are used as inputs of the system, which can be written as

$$\vec{x}_k = (x_1,\ y_1,\ z_1,\ x_2,\ y_2,\ z_2,\ x_3,\ y_3,\ z_3,\ x_b,\ y_b,\ z_b)^T,$$
$$\vec{z}_k = (x_1,\ y_1,\ z_1,\ x_2,\ y_2,\ z_2,\ x_3,\ y_3,\ z_3,\ s_{UAV1k},\ s_{UAV2k},\ s_{UAV3k})^T,$$
$$\vec{u}_k = (\Delta x_1,\ \Delta y_1,\ \Delta z_1,\ \Delta x_2,\ \Delta y_2,\ \Delta z_2,\ \Delta x_3,\ \Delta y_3,\ \Delta z_3,\ \Delta x_b,\ \Delta y_b,\ \Delta z_b)^T,$$

where $x_1,\ y_1,\ z_1$ are coordinates of first UAV, etc. $x_b,\ y_b,\ z_b$ are coordinates of the beacon, s_{UAV1k} is kth RSSI sample received by first UAV

and Δx_b, Δy_b, Δz_b are changes of beacon position in x, y, z directions, respectively.

Differential GPS modules are used to localize position of UAVs, therefore the first nine states are considered as precisely known. Because of that matrices $\mathbf{A}$, $\mathbf{B}$ are linear even identity matrices. Estimation of the last three states is highly non linear part of the system. The function $h(\vec{x}_k)$ that defines relation between position of UAVs, beacon and RSSI is

$$\vec{h}(\vec{x}_k) = \begin{pmatrix} x_{1k} \\ y_{1k} \\ z_{1k} \\ x_{2k} \\ y_{2k} \\ z_{2k} \\ x_{3k} \\ y_{3k} \\ z_{3k} \\ P_0 - 20\log(\sqrt{(x_{1k}-x_{bk})^2 + (y_{1k}-y_{bk})^2 + (z_{1k}-z_{bk})^2}) \\ P_0 - 20\log(\sqrt{(x_{2k}-x_{bk})^2 + (y_{2k}-y_{bk})^2 + (z_{2k}-z_{bk})^2}) \\ P_0 - 20\log(\sqrt{(x_{3k}-x_{bk})^2 + (y_{3k}-y_{bk})^2 + (z_{3k}-z_{bk})^2}) \end{pmatrix},$$

where P_0 is parameter that is defined in section 2.2.1, x_{1k} is x coordination of the first UAV at time k, etc.

2.4 Transmitting Beacon Model

The transmitting beacon needs to be simulated to test algorithms and system parameters. The beacon is defined by the current position and speed. In every step of the simulation, new RSSI sample is calculated for each of UAVs as:

1. Euclidean distance between the i-th UAV and the beacon is calculated from their positions as
$d_i = \sqrt{(x_b - x_{UAVi})^2 + (y_b - y_{UAVi})^2 + (z_b - z_{UAVi})^2}$.

2. The RSSI_i is obtained using equation (2.2) with information about distance d_i and determined parameter $P_0 = -36\text{dBm}$. Added noise is generated with Box Miller method with parameters corresponding to the noise described in section 2.2.2. Final RSSI is rounded, because resolution of XBee device is integer.

3. The RSSI_i value is published from model in the simulator to the i-th UAV.

This process is made 10 times in a second, which mimics a real beacon. If the distance d_i is smaller than 4 meters, the transmitting RSSI is set to -31dB. If the distance goes beyond 70 meters, the transmitting RSSI is set to $-\infty$.

Chapter 3

Formation Characteristics

In this chapter, it is described how the drones are organized into a formation such as in Figure 3.2. After that, in multiple tests, it is determined how the formation's relative position, rotation, size, and distance influence the precision of the localization of the beacon. These informations are used in the proposed localization algorithm.

Figure 3.1: Photo of the formation of the drones that is used to localize RFID.

3.1 Description

The formation of the UAVs is an organized group of vehicles. It stabilizes the UAVs relatively to ensure that there are no collisions during repositioning, at the same time, it simplifies control of the UAVs and ensures robust localization.

As mentioned in the Chapter 2 describing the system, position of each UAV is defined by Cartesian coordinates in three-dimensional space. However, to localize an object on ground only two coordinates are needed to be estimated - x, and y, thus only a planar formation is considered, meaning the surface containing all UAVs positions is parallel to the ground at a constant height. Default height of the formation is set to 5m to prevent collisions with objects on the ground. Moreover, to maximize directional stability, helicopters are evenly distributed on a circle in the formation.

The formation itself is defined by centroid C, radius r and angle θ_0 which corresponds to a rotation around the point C in a positive sense. As it can be seen in Figure 3.2, in case of 3 UAVs employed for the localization task positions of vehicles in the formation create an isosceles triangle. For $\theta_0 = 0$, the UAV_1 lies on the x-axis.

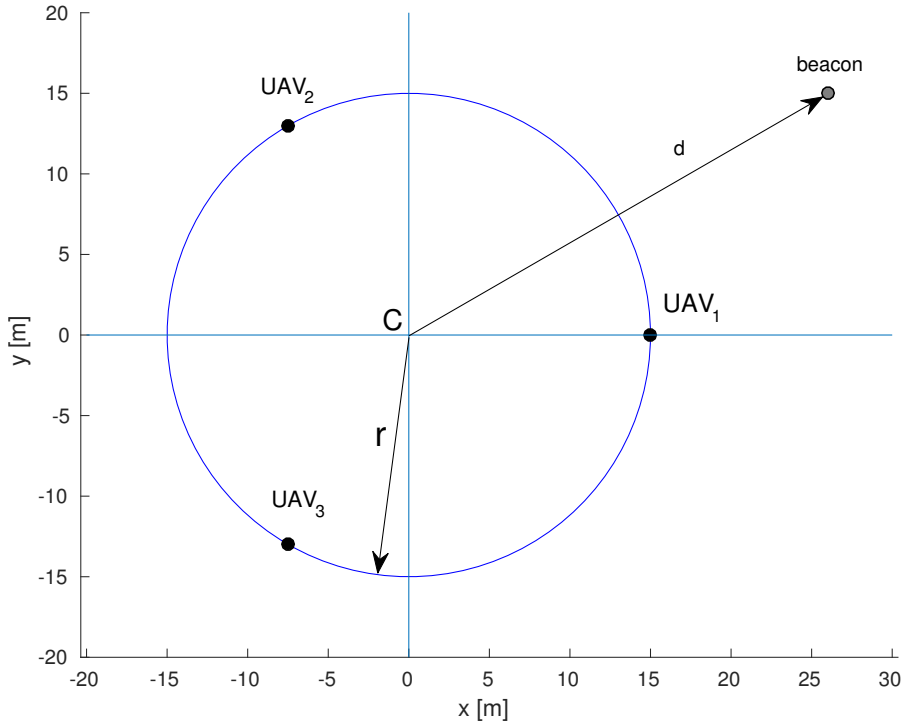

Figure 3.2: Schema of the formation with its parameters.

Position of the i-th helicopter is determined by position of the center and

the radius of the formation as

$$\begin{aligned} x_{UAVi} &= x_C + r\cos(\theta_i + \theta_0), \\ y_{UAVi} &= y_C + r\sin(\theta_i + \theta_0), \\ z_{UAVi} &= c_z, \end{aligned}$$

where x_C, y_C are coordinates of the center, r is the radius of the formation, c_z is the height of the formation, θ_0 is the offset and θ_i can be computed for the i-th drone as

$$\theta_i = \frac{i-1}{n}360,$$

where n is the total number of UAVs, in this work $n = 3$. It is a minimal number that the used algorithms are able to localize the transmitter with. θ_i is an angle in [deg] which is measured around C in the positive direction starting from x-axis.

3.2 Relative Position

A simulation for different beacon positions is done to test how the relative position of the formation with respect to the transmitter influences the accuracy of the estimation.

As shown in section 2.2.1, the maximal distance from the transmitter to the receiver at which the communication still works is about 70m. Hence, a square with 80m edge is considered as an active area around the formation. The active area is part of the workspace with high probability that all of the UAVs capture signal from the beacon. A localization error for 6400 positions, which are computed as a distance between the actual and averaged estimated position is shown in the Figure 3.3. An average estimated position is calculated from 1000 estimated positions obtained by simple triangulation algorithm, which is described in section 4.1, to suppose the noise.

Parameters of the formation used in the simulation are static and they are set as

$$\begin{aligned} x_C &= 0, \\ y_C &= 0, \\ \theta_0 &= 0, \\ r &= 15m. \end{aligned}$$

The positions of the beacon are generated evenly spaced in a square formed points $[-40,\ -40]$, $[-40,\ 40]$, $[40,\ -40]$, $[40,\ 40]$ with a 1m step.

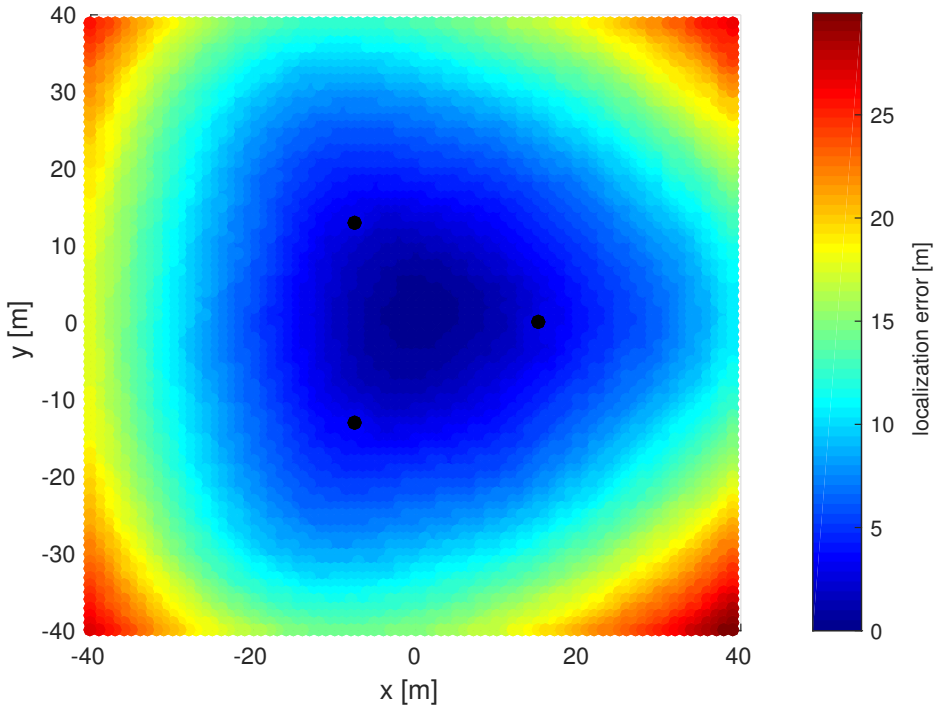

Figure 3.3: Localization error in active area. One thousand samples are simulated and avereged for each position.

The Figure 3.3 shows that relative position of the formation and the beacon highly affects the precision of the estimated position. As it can be seen, the best results (the smallest error) are achieved inside of the formation with the best localization precision being about 0.4m. Inaccurate estimation at the corners of the active area are caused by mirroring points, as it is written in section 4.1.

3.3 Parameters Testing

Each of the parameters independently is examined in the following tests. It is done to determine which and how each of the parameter affects precision of the estimation.

3.3.1 Size

The first tested parameter is the size of the formation, represented by the size of radius r. In the simulations, the beacon is placed in the center of the formation, so coordinates of the transmitter $[x_b,\ y_b] = [0,\ 0]$. The radius is increased by 0.1m in each step from 5 m to 35 m. Again, 1000 estimated

positions are obtained for each step by simple triangulation method. The data are then averaged, and error is calculated as a difference between the estimated and the actual positions.

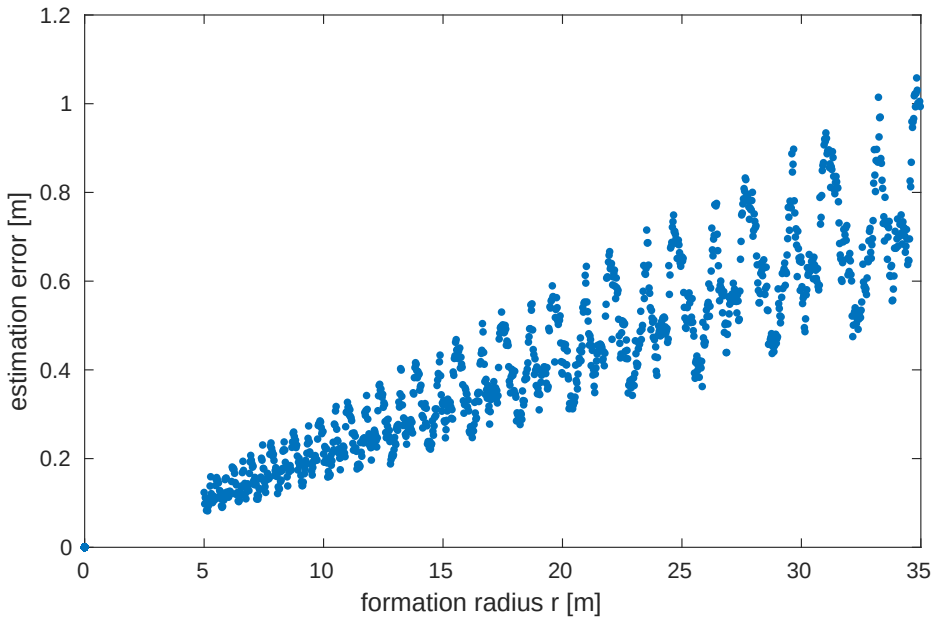

Figure 3.4: Error of the localization depending on the radius size of the formation in case that the beacon is in the center of the formation.

As it can be seen in Figure 3.4, with bigger radius the error increases as well as its diffusion. The best estimation of position is when the formation has the smallest possible radius.

3.3.2 Rotation

In the second test, it is measured how the precision of the localization depends on the angle θ_0. In other words, it is measured how the rotation of the formation influences the estimation of the position. Distance d between a center of the formation and the beacon is constant 30m. Transmitter is placed at $[x_b,\ y_b] = [30,\ 0]$ and the formation rotates by 0.5 degree in each step.

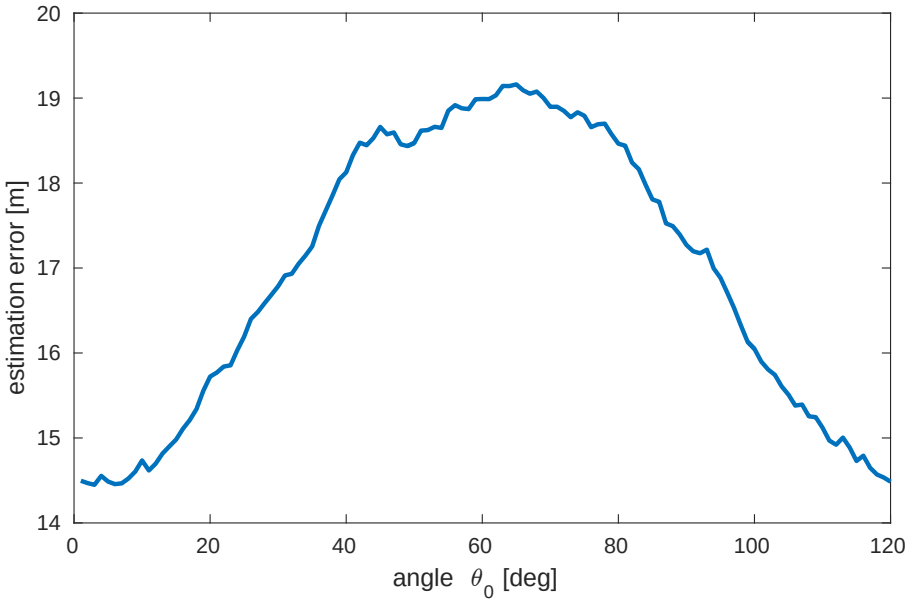

Figure 3.5: Depandance of the localization error of the localization on the rotation of formation.

Localization precision is surprisingly influenced by the rotation. As it can be seen in Figure 3.5, the difference goes up to 20%. The worst results are obtained for $\alpha \approx 60\,\text{deg}$, which is a configuration where the beacon was on a line starting in the center of the formation and leading between UAV_1 and UAV_2.

3.3.3 Distance

In the last test, the formation position and parameters are $C = [0,\ 0]$, $\theta_0 = 0$, $r = 15m$. The beacon is shifted on the x-axis. Tested x position of the beacon is ranging again from -40 to 40m.

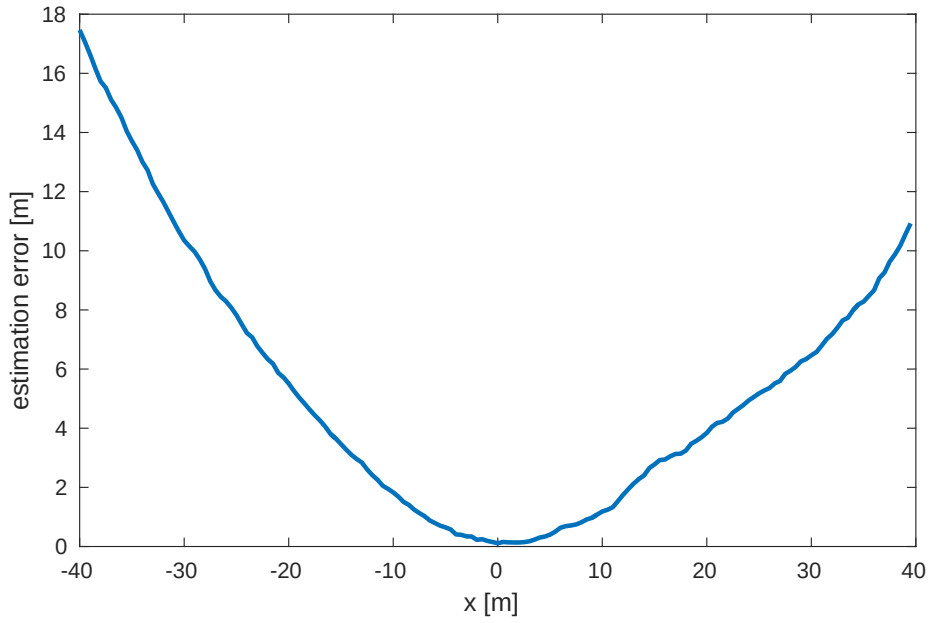

Figure 3.6: Localization error according to position of the beacon on the x-axis. Center of the formation is [0,0].

This test confirms that the best estimation is obtained for the positions of the beacon in the center of the formation. The smallest error is about 0.25m and the biggest error 17.5m, which can be seen in Figure 3.6.

3.4 Resume

Based on the initial experiments described in this chapter, it can be concluded that the best estimation of the seeking beacon position is if the estimated position is in the center of the formation and the size of the formation is the smallest as possible. Furthermore, if the estimated position can not be reached by the formation, localization can be made more accurate by rotation of the formation based on current estimation of of direction of the beacon.

Assuming that the maximal possible distance from the transmitter to receiver is about 70 meters, it also means that if the radius of the formation is $r = 70$m, the active area is exactly one point in the center of the formation. On the contrary, if the radius is $r = 5$m, the active area is almost circle with approximately 65 meters radius. But at the same time, almost whole

active area is outside of the formation. Both of the mentioned set-ups are the extreme cases. However, finding optimal balance between speed of searching (which is affected by the size of the formation) of the area and the precision of the estimation (which is mostly affected by the relative position to the formation) can be examined in the future work.

The conclusions presented in this chapter are used in the state machine that is used to localize a static beacon that is described in section 4.4.

Chapter 4

Localization Algorithms

Two types of algorithms are used to localize the transmitting device. The first, simple method is based on single measurement triangulation. It is described in section 4.1. As it turns out, this approach is very inaccurate because of the strong influence of the RSSI noise. It is assumed that this noise has a normal distribution with zero mean, so triangulation algorithm is expanded to perform averaging of received signal strengths to eliminate this problem. More information about so-called sequential triangulation is in section 4.2.

The second method is using Unscented Kalman filter, which is described in section 4.3. It is an optimal recursive algorithm that can be used to estimate states from the system with a nonlinear function, such as equation (2.2). The needed state-space model of the system is defined in section 2.3. Moreover, this approach can be used to predict a position of a moving beacon. If there is aprior knowledge about the movement, it can be set as an input into the system. On the other hand, this algorithm has to be initialized with estimation of states and covariance which is subjected to an inaccuracy of assessment.

Possible localization scenarios can be divided into two options. The first one is finding a position of a static beacon. The best autonomous estimation of the beacon position is made with a state machine which combines both above-mentioned algorithms (sequential triangulation and UKF). This option is described in section 4.4. The second option is tracking the position of a moving beacon. In this case, there are two types of algorithm - simple triangulation with floating window, or UKF. Their comparison is made in section 5.1. All approaches can be decentralized so that each of the UAV runs the same algorithm only with the difference that each UAV has set its position in the formation. Each of the UAV streams an RSSI and current position to the rest of the group and synchronization confirmation is done after each measurement is received to keep stability.

4.1 Triangulation

With a presumption that the beacon is always on the ground, a problem of localization is reduced to 2D. Three different positions with estimated distance to the beacon are needed to reach the point on the plane. It is expected that in one iteration there are RSSIs from all three UAVs known. Distance between transmitter and receiver on the UAV can be calculated from RSSI, according to equation (2.2) as

$$R = 10^{\frac{P_r - P_0}{-20}}, \tag{4.1}$$

where calculated distance is in [m], P_r is received power in [dBm] and P_0 is parameter determined in section 2.2. When the distance is estimated, it is known that beacon lies somewhere on a circle with a radius R and with center equal to the current position of the UAV. The distances from other two UAVs are calculated in the same way. Under ideal conditions, all three circles would intersect in the exact point, which would be the position of the transmitter. But under real-world conditions we expect noise. Moreover, used XBee devices have only integer resolution of RSSI. Therefore, it is assumed that all three circles do not intersect in one point, such case can be seen in the Figure 4.1.

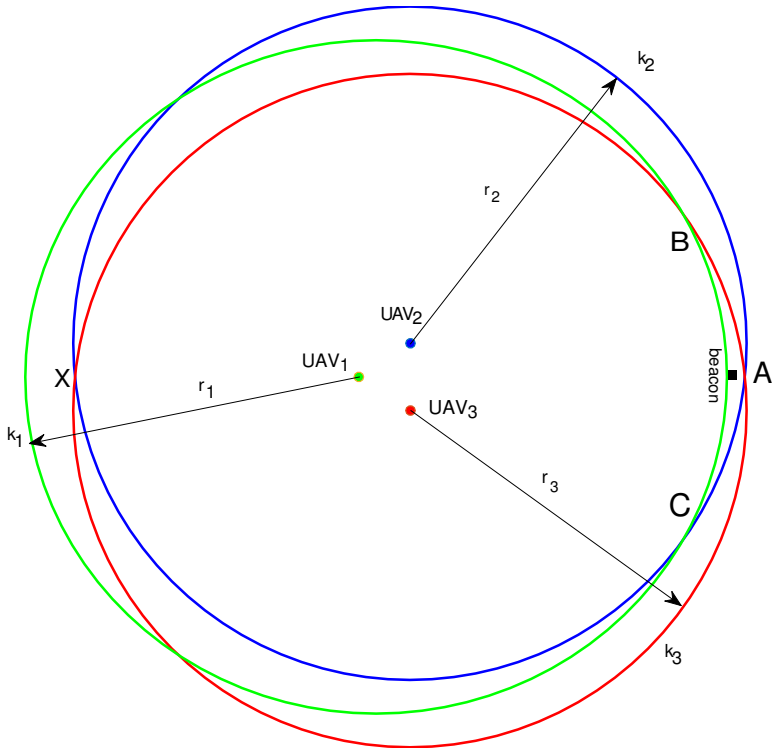

Figure 4.1: The UAV formation with circles k_1, k_2, k_3 that represent distance accounted from measured RSSI. And possible intersections of the circles.

The algorithm computes intersections of a pair of circles. If there is no intersection found, the algorithm continues with another pair of circles. Further, if there is one intersection, this point is accounted. Otherwise, if two intersections of circles is found, which is the most common case, the algorithm decides which one to use based on the distance from the last UAV. For example circles k_2, k_3 with centers in UAV_2 and UAV_3 respectively intersect in two points, specifically in points A and X in Figure 4.1. Point A is selected from the two because

$$|r_1 - |AS_{UAV1}|| < |r_1 - |XS_{UAV1}||,$$

where $|AS_{UAV1}|$ is a size of line segment consisting of points A and S_{UAV1} and r_1 is a radius of the circle k_1.

There are three possible pairs of circles k_1, k_2 and k_1, k_3 and k_2, k_3. The maximal number of points, that are selected by the above mentioned rules, are three (one from each of the pair of circles). If there is none point selected, current iteration is unused. If there is only one point selected, it is assumed to be the estimated position. Otherwise, estimation of beacon position is computed as an average of all points if there are two or three points selected. In the example (Figure 4.1) there are three points determined, namely A, B, C, therefore, estimation of position would be center of gravity of the triangle formed by these points.

The biggest estimation error is caused by selection of a wrong point by the algorithm. The case could be that due to noise the point X is taken instead of point A, and same for the other points. Thus the estimated position is mirrored to the second half-plane from the formation.

1000 iterations are simulated for 6400 positions evenly distributed in an area 80m×80m with the formation in the middle, to define estimation error. Average estimation error (Euclidian distance between true and estimated position) is 35.64m, which is a very weak outcome. A sliding window average is employed to make this algorithm more robust. The estimations are put into a stack with fixed maximal size. With a new iteration the estimate is inserted onto the top, and when the stack is full, the oldest estimation is thrown away. Final estimation is made each time as an average of positions in the stack.

4.2 Sequential Triangulation

Under assumption that the noise of RSSI has a normal distribution with zero mean, averaging of RSSI values over time and triangulation performed afterward reduce estimation error. The probability of so-called mirroring (described in sec. 4.1) is quickly reduces with an increasing number of samples. However, the formation of UAV must be static during one sequence

of measurements. Furthermore, this approach can be applied only to static transmitter or slowly moving.

A disadvantage of this extension is that information about history of measurements has to be known. To protect overflow of the variables, averaged RSSI value is computed as

$$s_i^{avg} = s_{i-1}^{avg} + \frac{(s_{received} - s_{i-1}^{avg})}{i_s},$$

where, $s_{received}$ is current received signal strength sample, $i_s \in < 1, i_{max} >$ is the number of the sample and i_{max} is the maximal number of samples in a sequence.

To test an improvement of the algorithm, 1000 sequences with 100 measurement samples are simulated for each of the positions throughout the area. As it can be seen in Figure 4.2, the average error is rapidly reduced with more samples.

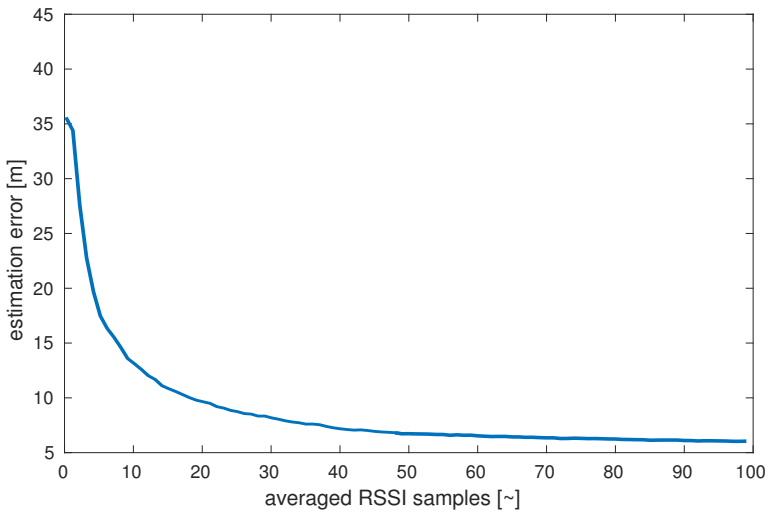

Figure 4.2: Average error estimation according to the number of samples in sequence.

On the one hand, this approach is much more robust and precise than a single measurement triangulation. The mean of the error is reduced under the half with averaged ten samples. On the other hand, this approach is more time consuming and conditioned with a static position of both the formation and the transmitter. Thus it cannot be used for a localization of a moving device.

4.3 Unscented Kalman Filter

Kalman filter is an algorithm that consists of two phases - prediction step and update step. It estimates an unknown variable over time. It has an advantage that only the estimated states from the previous time step and current measurement are needed to be known. The filter is a recursive algorithm, therefore, history of samples of estimations and measurements is not required. But initialization of the states including estimated ones along with a covariance is needed. Furthermore, the system model is also needed. It is described in section 2.3. Each of the states is represented by mean and uncertainty which is called covariance.

Unscented Kalman filter is used in this work to estimate the position of a moving beacon with aprior information about its speed.

Due to a nonlinear function $h(\vec{x})$, the basic Kalman filter could not be used. Two types of Kalman filter are used with nonlinear systems - Extended Kalman filter and Unscented Kalman filter. Extended Kalman filter can give a poor quality of estimation due to a linearization of a highly nonlinear function such as in this case exponential function (4.1). Therefore, Unscented Kalman filter is chosen for this work. In this case, it offers better performance and robustness.

So-called unscented transformation is used to deal with non-linear functions in the system. Set of points, called sigma points, are chosen from surroundings around mean value of the state and they are propagated through that function.

4.3.1 Prediction Step

Number of the sigma points equals to $2L + 1$, where L is a number of states in the system. The first sigma point is exact mean of the state and others can be divided to positive and negative points, they are derived from state vector and covariance as

$$\begin{aligned}
\chi^0_{k-1} &= \vec{x}_{k-1}, \\
\chi^i_{k-1} &= \vec{x}_{k-1} + (\sqrt{(L+\lambda)\mathbf{P}_{k-1}})_i, \qquad i = 1, ..., L \\
\chi^i_{k-1} &= \vec{x}_{k-1} - (\sqrt{(L+\lambda)\mathbf{P}_{k-1}})_{i-L}, \qquad i = L+1, ..., 2L
\end{aligned}$$

where $\vec{x}_{k-1}$ is a state vector, $\mathbf{P}_{k-1}$ is the covariance and λ is a constant that can be defined as a

$$\lambda = \alpha^2(L + \kappa) - L,$$

where α and κ are constants, described in 4.3.3.

Each of the sigma points is then propagated through the system model and can be determined from the system matrix, the input matrix, the input vector and the sigma points themselves as

$$\chi_k^i = \mathbf{A}\chi_{k-1}^i + \mathbf{B}\vec{u}_k,$$

which is described in section 2.3. New predicted state vector and covariance are determined from these weighted points as

$$\hat{\vec{x}}_k = \sum_{i=0}^{2L} W_s^i \chi_k^i,$$
$$\hat{\mathbf{P}}_k = \sum_{i=0}^{2L} W_c^i [\chi_k^i - \hat{\vec{x}}_k][\chi_k^i - \hat{\vec{x}}_k]^T + \mathbf{R},$$

where $\mathbf{R}$ is a process covariance matrix described also in section 2.3. Weights are accounted as

$$W_s^0 = \frac{\lambda}{L+\lambda},$$
$$W_c^0 = \frac{\lambda}{L+\lambda} + (1 - \alpha^2 + \beta),$$
$$W_s^i = W_c^i = \frac{\lambda}{2(L+\lambda)},$$

where W_s^0 is weight of sigma point that corresponds to the mean of the state, W_c^0 is a weight of covariance of the same point, W_s^i is weight of others sigma points and β is a constant described also in 4.3.3.

Sigma points are propagated through non-linear $h()$ function to predict output of the system. Such as

$$\Upsilon_k^i = h(\chi_k^i).$$

And finally, predicted measurement vector of the system can be obtained as

$$\hat{\vec{y}}_k = \sum_{i=0}^{2L} W_s^i \Upsilon_k^i.$$

4.3.2 Update Step

Correction of the estimated output is made in the update step with measurements. The predicted measurement covariance matrix and the state measurement cross covariance matrix are required to compute Kalman Gain. Covariances are written as

$$\mathbf{P}_{yy} = \sum_{i=0}^{2L} W_c^i [\Upsilon_k^i - \hat{\vec{y}}_k][\Upsilon_k^i - \hat{\vec{y}}_k]^T + \mathbf{Q},$$
$$\mathbf{P}_{xy} = \sum_{i=0}^{2L} W_c^i [\chi_k^i - \hat{\vec{x}}_k][\Upsilon_k^i - \hat{\vec{y}}_k]^T,$$

where $\mathbf{Q}$ is a measurement covariance matrix and weights equal to those from prediction step. Then, Kalman gain is computed as

$$K = \mathbf{P}_{xy}\mathbf{P}_{yy}^{-1}.$$

The correction of the mean of each of the states and its covariance is updated as

$$\vec{x}_k = \hat{\vec{x}}_k + K(\vec{y}_k - \hat{\vec{y}}_k),$$
$$\mathbf{P}_k = \hat{\mathbf{P}}_k - K\mathbf{P}_{yy}K^T,$$

where $\vec{y}_k$ is a measurement vector and $\hat{\vec{y}}_k$ is a predicted measurement vector from the prediction step. Afterward the estimation is done. The whole process can be computed again with a new input and a new measurement again in the next iteration.

4.3.3 Parameters

During the initialization of the Unscented Kalman filter parameters, such as a constant that influences the spreading of sigma points around the mean of each of the state, have to be set. The parameters are set to

$$\alpha = 0.01,$$
$$\kappa = 0,$$
$$\beta = 2,$$

which are standard values, when the distributions of $\vec{x}$ are Gaussian (normal) distributions. Measurement and process noise covariance matrices are set to

$$\mathbf{Q} = \begin{bmatrix} 0.1 \cdot \mathbf{I}_{9\times9} & \mathbf{0}_{9\times3} \\ \mathbf{0}_{3\times9} & 2.5 \cdot \mathbf{I}_{3\times3} \end{bmatrix},$$

$$\mathbf{R} = \begin{bmatrix} 0.1 \cdot \mathbf{I}_{9\times9} & \mathbf{0}_{9\times3} \\ \mathbf{0}_{3\times9} & \mathbf{0}_{3\times3} \end{bmatrix}.$$

As an all state measurement, precise covariance is set small and the covariance of RSSI measurement is set as a deviation of the normal distribution of noise described in section 2.3. Initial position and covariance are set in each simulation and experiment specific.

4.4 State Machine

A finite state machine can be used to find and localize a static transmitter, which can be seen in Figure 4.3. It combines the two approaches - sequential

measurement (section 4.2) and UKF (section 4.3). First, a rough estimation of beacon position is found by sequential measurement. The formation is then moved to have the estimated position in the center while the radius of the formation is also made smaller. Afterwards, more iterations of the same steps are done until the changes of estimated position are under a threshold.

The used XBee devices have an integer resolution of received signal strength. In the case that the smallest possible size of formation is $r = 5$m, the Euclidian distance between transmitter and receiver is approximately 7m when the beacon is in the middle of the formation and altitude of the formation is 5m. The RSSI that corresponds to this distance (according to the equation 2.2) is about -53dBm. Value -54dBm corresponds to the distance 7,94m. It means that resolution of determining the distance from RSSI is about 0.9m at best. For example, the resolution at a 30m distance between transmitter and receiver equals to the 2.7 meters. Therefore, the formation is moving in a shape of a letter 'X' to improve estimation. And because the formation is moving, the UKF is used.

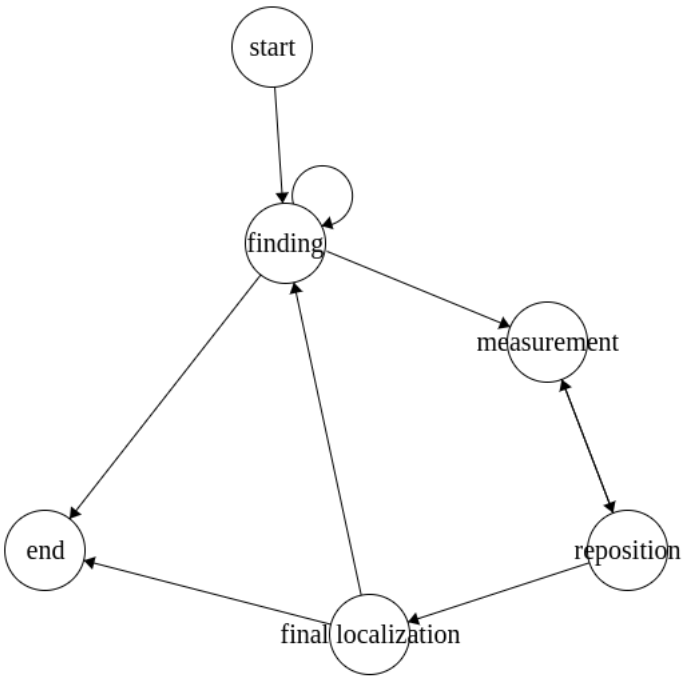

Figure 4.3: Finite state machine diagram, which is developed on a results from Chapter 3.

The first state is called *finding*, and it consists of scanning the desired area. The type of scanning may vary depending on the specified conditions. For example, each of UAV can seek through the separate part of the area

with gradient estimation. Alternatively, all UAV formed in the formation can search area in so-called 'lawn mower' pattern. (Comparison of performance and difference scanning algorithms could be examined in the future works.) Algorithm stops and formation is returned to the start if the UAVs do not receive any signal in the whole area. Otherwise, the state machine is changed to *measurement* state when the signal from the known device is captured. In this state, the sequential triangulation (described in section 4.2) algorithm is used. As is determined in Chapter 3, the best position is estimated when the transmitter is in the center of the formation. Therefore, after *measurement* state, the next state of the state machine is *reposition*, in which the formation is moved to get its center at the estimated position from the previous state. Then the state machine is changed to the *measuremant* state again. If the new estimation is close to last one, in other words, estimation remains in the middle of the formation, the radius of the formation is reduced in the next *reposition* state, to improve localization (according to section 3.3.1).

When the formation is at minimum size (which means the smallest possible radius) final estimation is obtained from state $final\ localization$ by UKF, which is initialized with estimation from sequential triangulation. Moreover, the formation is moving in the surroundings to receive RSSIs from different positions to improve estimation.

So final estimation of the beacon is assigned. The formation is continuing to localize another beacon, or it is returned to the starting point if there is no other device in the area.

Chapter 5

Simulated Experiments

The goal of the simulations is to test and compare the developed algorithms. Simulations are made in Gazebo simulator under ROS which offers similar conditions to a real world, with one difference that the received signal is generated by a model described in section 2.4. By using the Gazebo simulator, the time needed to proceed from simulations to experiments is significantly reduced.

Two types of set ups of localization are created. The first one (in section 5.1) is an estimation of the moving beacon with the static formation. The second scenario is opposite (in section 5.2), static transmitter is localized by the moving formation.

5.1 Moving Transmitter

A position of a moving beacon is estimated in the first simulation. In Figure 5.5 is series of snapshot from simulator. The whole simulation can be seen at youtube[1].

The formation is static with parameters corresponding to

$$\begin{aligned} x_C &= 0, \\ y_C &= 0, \\ r &= 15m, \\ \theta_0 &= 0. \end{aligned}$$

Beacon is moving with linear straight motion during the whole simulation. The starting point is $[-20,\ -10]$ and the end point is $[40,\ 20]$. Speed of movement is $v = 22.36ms^{-1}$. Trajectory of the movement can be seen in Figure 5.1.

[1] `https://youtu.be/FZvavgReAIc`

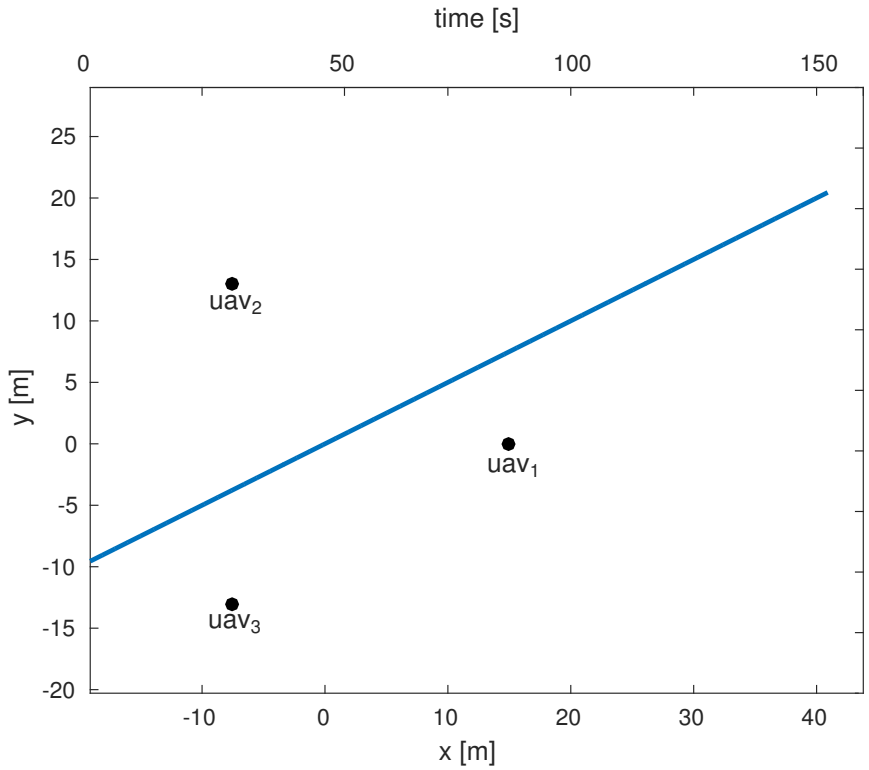

Figure 5.1: Trajectory of a linear movement of the beacon in x,y space. Denoted static position of the formation.

Two types of algorithm are tested. First is triangulation with a sliding window of 30 samples. Localization error over time can be seen in Figure 5.2. With ten samples per second and the need of thirty samples size of sliding window, averaged samples are obtained over three seconds, during that time beacon shifts for about 0.67m.

The second algorithm is the UKF with a-priori knowledge about the direction of the movement. The UKF states are initialized with first nine states as current positions of drones. And the estimated position of the beacon is initialized as $[0, 0, 0]$ which corresponds to the center of the formation. Localization error over time can be seen in Figure 5.3.

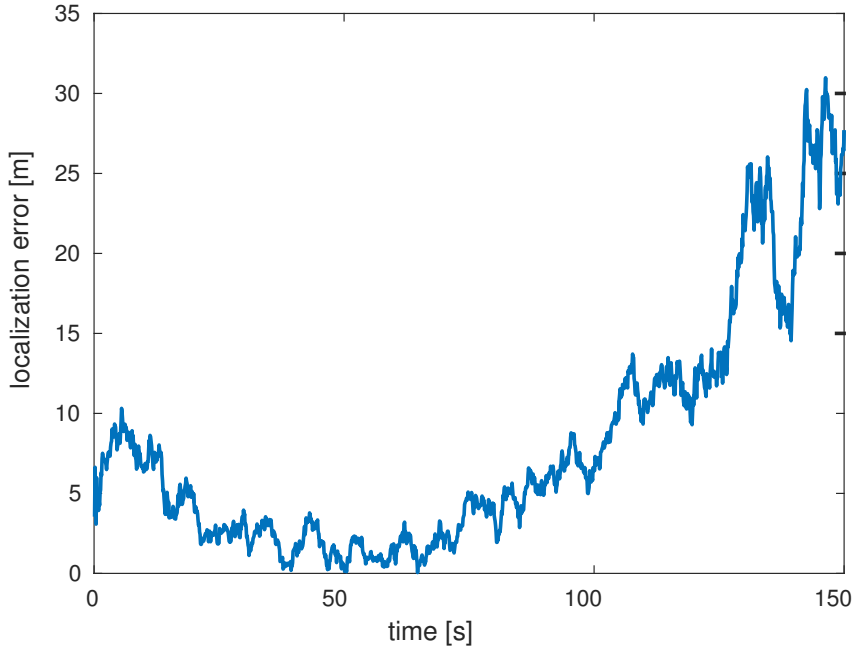

Figure 5.2: Localization error of the moving transmitter over the time. Estimation made by triangulation algorithm with the floating window with 30 samples.

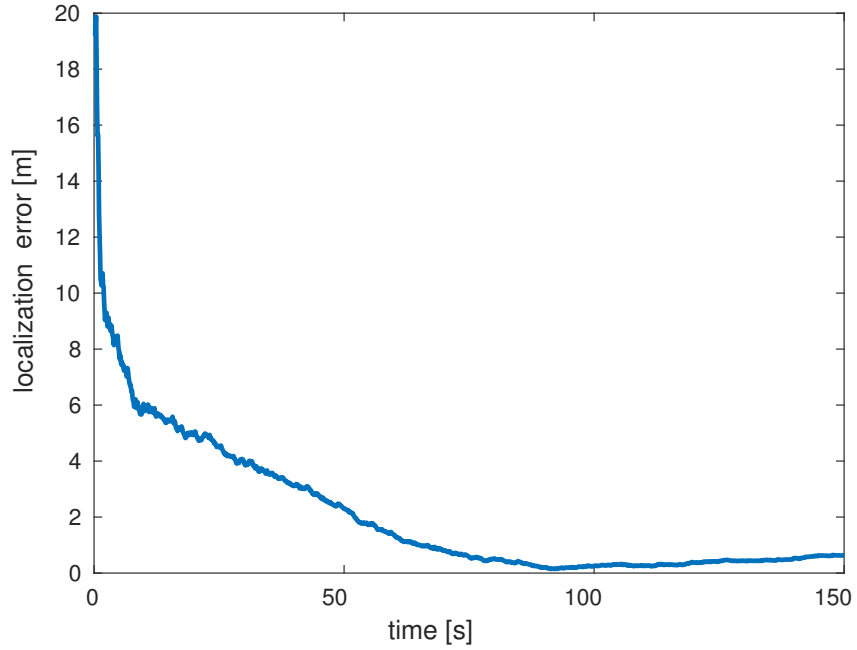

Figure 5.3: Localization error of the moving transmitter over the time. Position is estimated with the Unscented Kalman Filter with the a-prior movement information.

As can be seen in the Figure 5.2, the best estimation by the first approach is when the moving beacon is in the center of the formation, estimation error is there about 0.74m. As the beacon goes out of the formation, estimated precision is rapidly reduced, that confirms findings from Chapter 3.

The UKF with a-prior knowledge performs better results. Due to poor initialization, it takes time to converge, but after that its relative position is less conditional from the view of the formation. On the other hand, if there is no apriori knowledge about beacon speed, estimation is much worse. That is simulated as well, and can be seen in the figure 5.4.

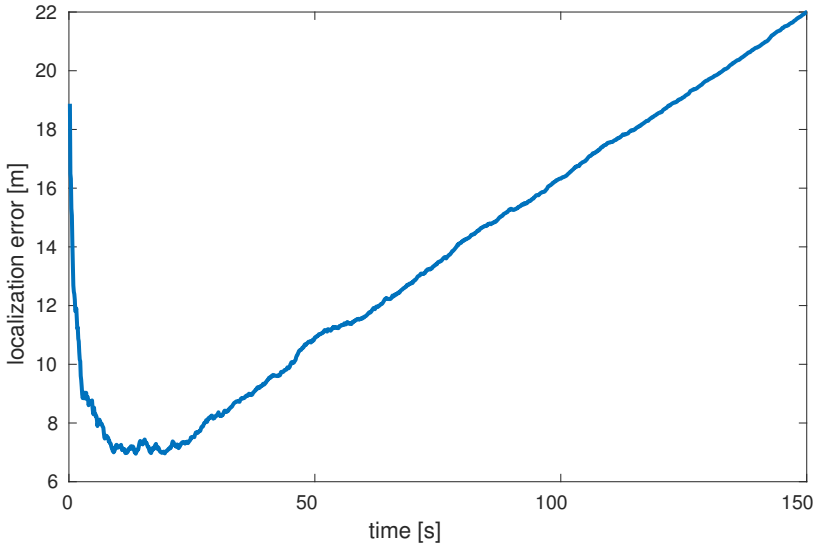

Figure 5.4: Localization error of the moving transmitter over time. Position of beacon estimated with the Unscented Kalman Filter with the wrong a-prior movement information.

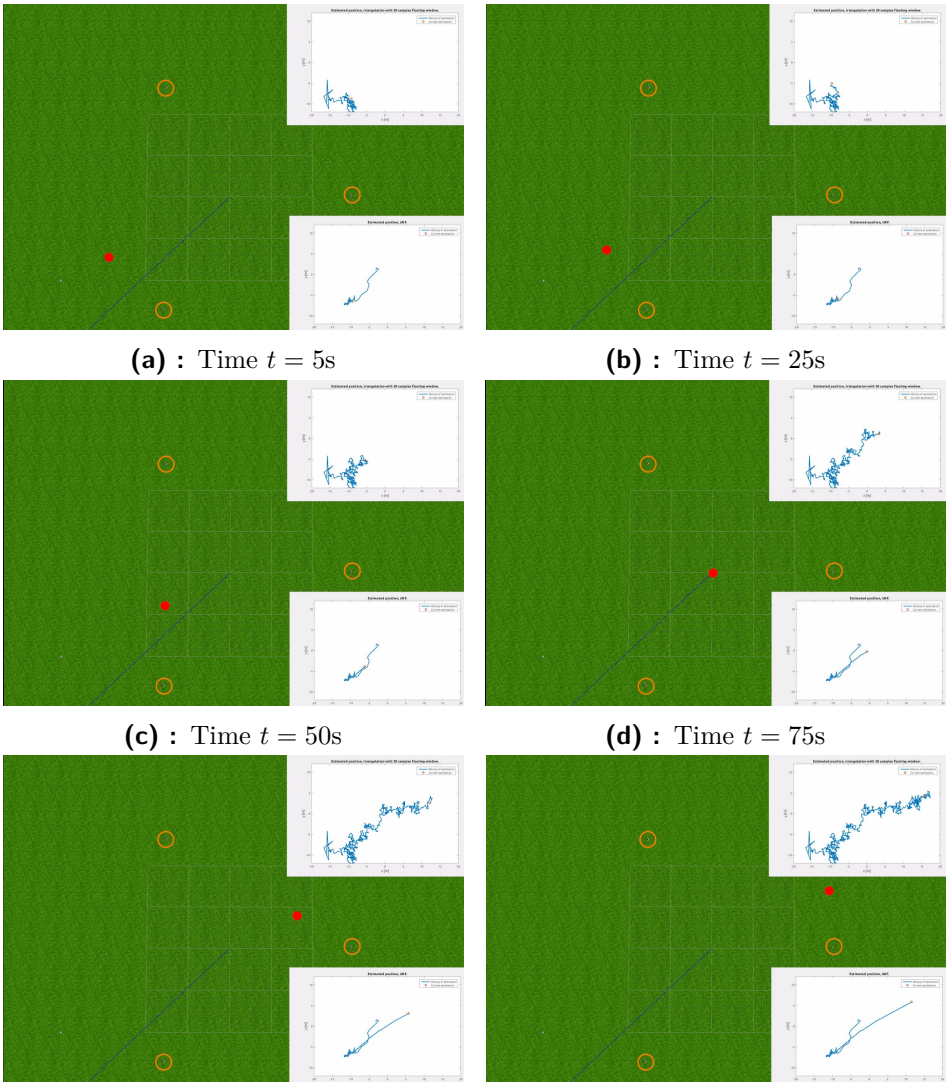

(a) : Time $t = 5$s **(b) :** Time $t = 25$s

(c) : Time $t = 50$s **(d) :** Time $t = 75$s

(e) : Time $t = 100$s **(f) :** Time $t = 125$s

Figure 5.5: Snapshots from simulator, localization of a moving beacon. Red dot represents beacon.

5.2 Static Transmitter

The second simulation aims to test the localization of the static transmitter. Used approach is described in section 4.4 which combines two algorithms, the sequential triangulation, and UKF. A number of samples in one sequence (one estimation iteration) is set to 20. To achieve the best estimation, the formation whirls during the final estimation by UKF. In Figure 5.9 are shown snapshots from simulator during localization of a static beacon. Whole simulation can be seen at youtube [2].

[2] `https://youtu.be/Ym40Cn0--E8`

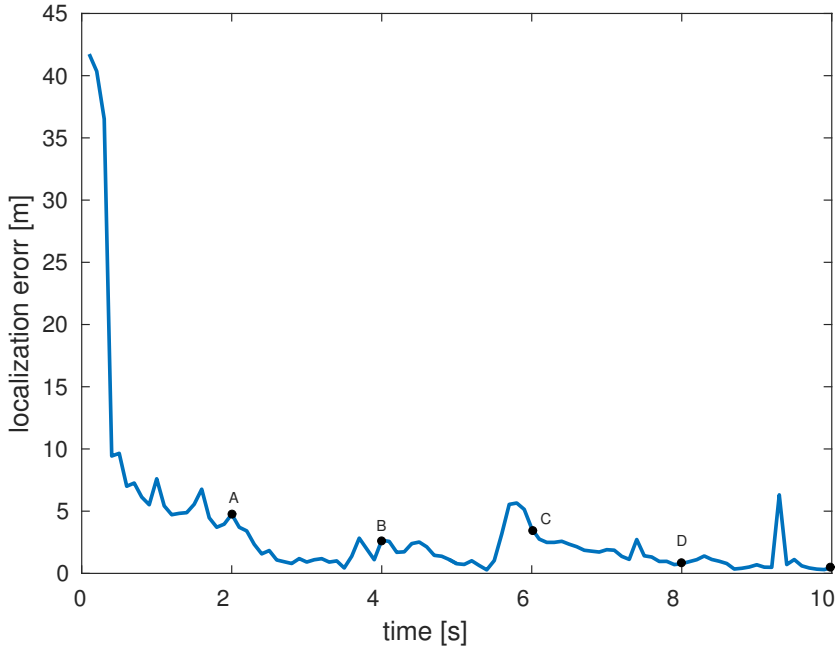

Figure 5.6: Localization error of the static transmitter over the time. Position is estimated by the sequential triangulation with twenty samples large sequence.

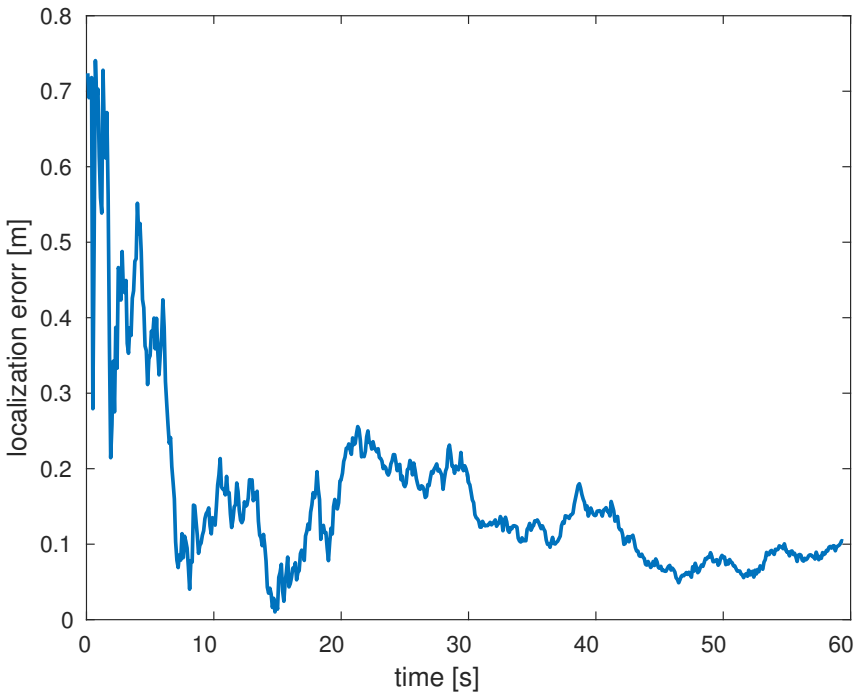

Figure 5.7: Localization error of the static transmitter over the time. Estimation of position made by Unscented Kalman Filter.

At the time corresponding to points A, B, C and D in the Figure 5.6, formation is repositioned. After A, center of formation is changed from $[0,\ 0]$ to $[40.7,\ 41, 46]$, at B to $[44, 9, 45.2]$, where it stays. At point C and D formation reduced its radius about 5 meters. The time that the formation flies to another position has not been plotted, because during the *reposition* state no RSSI is measured. The error of estimated position after the sequential triangulation is 0.73m.

After that, estimation from sequential triangulation is set as an initialization of the UKF. Covariance of this estimation is set as 2.57 which corresponds to the standard deviation of the measured noise of the RSSI, which is described in 2.3. As can be seen, another 600 samples are measured with the UKF. Resolution of the RSSI of used antenna is integer. Therefore, formation flies in an "X" around estimated position to get more distributed RSSI data, during final localization. Trajectory of this movement can be seen in Figure 5.8.

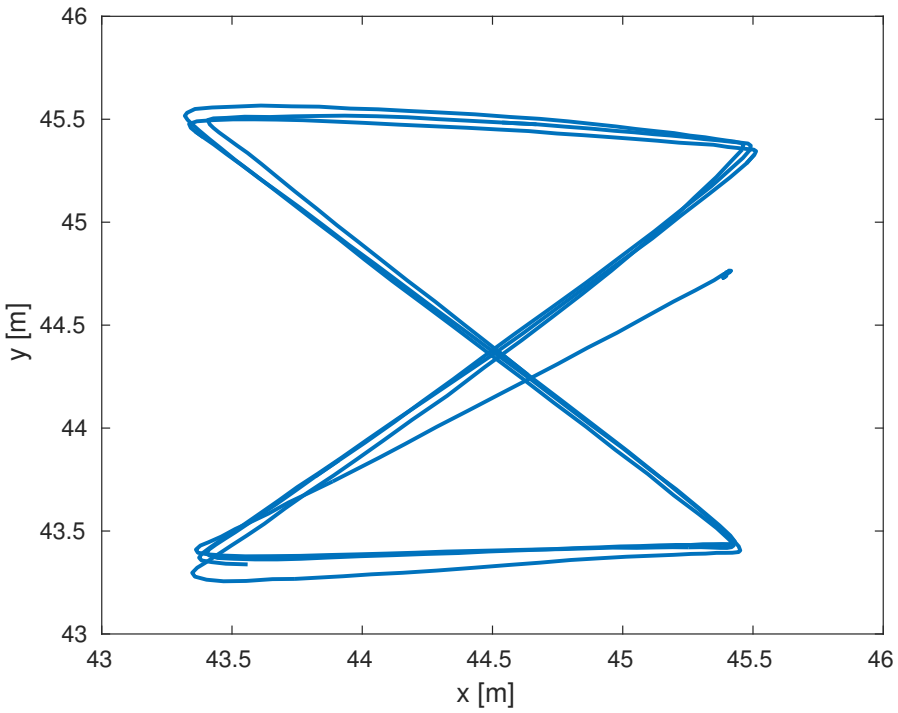

Figure 5.8: Formation trajectory during final localization.

As shown in Figure 5.7, with this approach, position of the beacon is estimated with excellent accuracy. Estimation error is only about 0.1m after 400 samples.

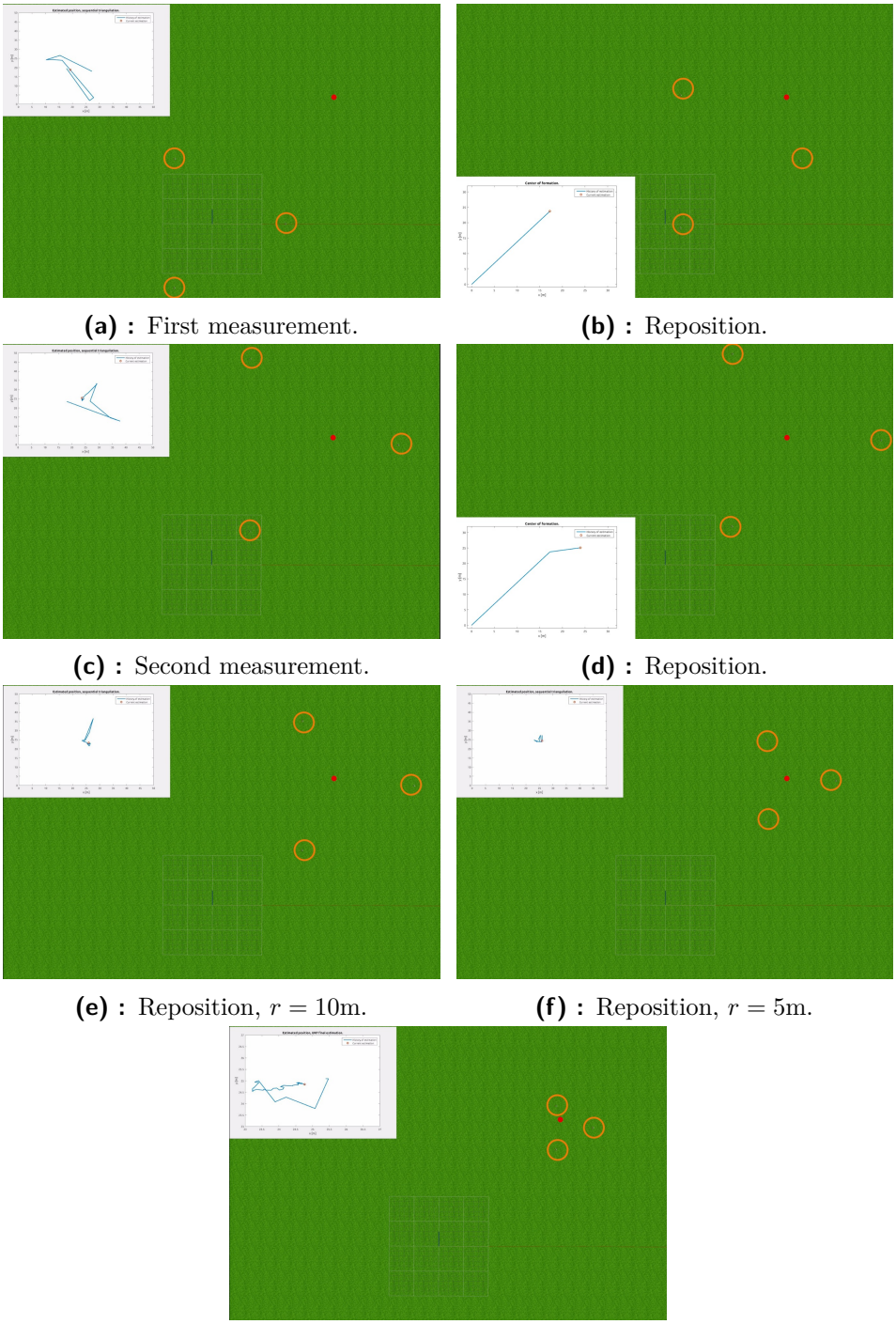

(a) : First measurement. **(b) :** Reposition.

(c) : Second measurement. **(d) :** Reposition.

(e) : Reposition, $r = 10$m. **(f) :** Reposition, $r = 5$m.

(g) : UKF final localization.

Figure 5.9: Snapshots from simulator, localization of a static beacon. Red dot represents beacon.

Chapter 6

Real Experiments

The approach presented in this thesis is tested in the real-world experiments. Additionally, usability and robustness of the XBee devices as a radio frequency communication platform is examined as well.

First, the parameters of the received signal (described in section 2.2) are measured. As mentioned in section 2.2.1, it is assumed that parameter $n = 2$, which is a value that corresponds to a free-space path loss.

Next, to measure RSSI characteristic over a distance between receiver and transmitter, it is needed to assess the parameter P_0. The RSSI depends highly on the receiver. Therefore, the dependence of the signal strength on the distance to the transmitter is measured for each of the receiving antenna separately. One transmitting beacon is laid on the ground on a known position.

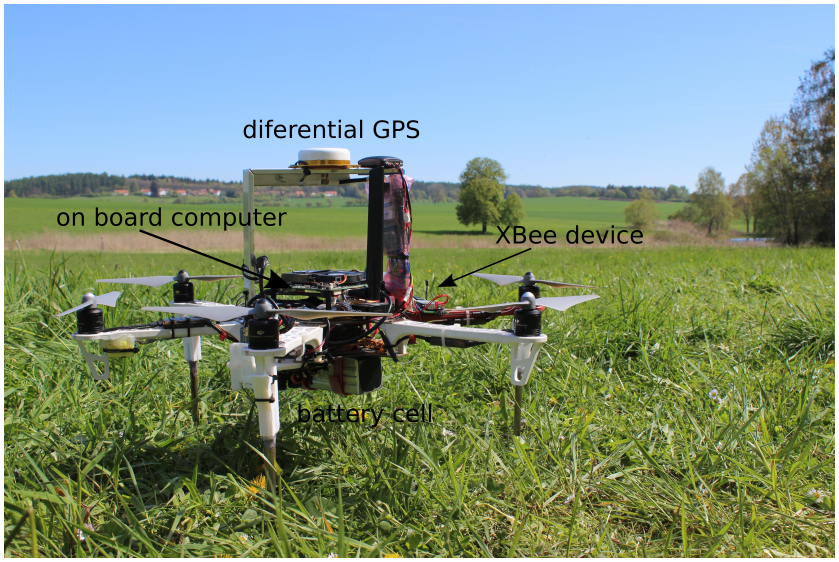

Figure 6.1: UAV with on board sensors.

The receiver is put on the drone which flies at a 5m altitude in the surroundings of the beacon. Used UAV is shown in Figure 6.1. Obtained data from each of the antenna are shown in the next figures 6.2, 6.3, 6.4. They correspond to the antenna on the UAV_1, UAV_2, UAV_3, respectively. Process of measurement can be seen in Figure 6.6.

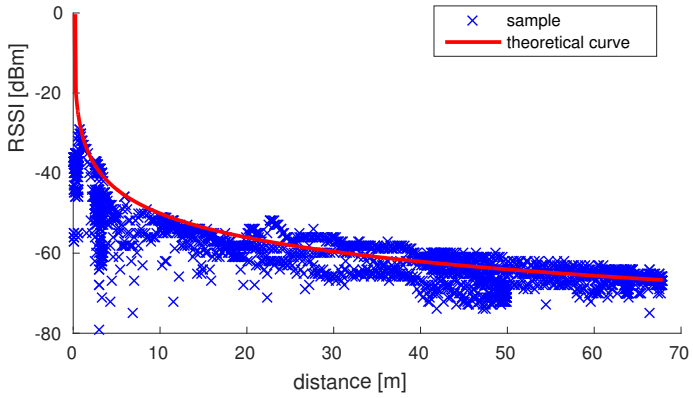

Figure 6.2: Measured RSSI samples depending on a distance with fitted theoretical curve. Antenna on the UAV_1.

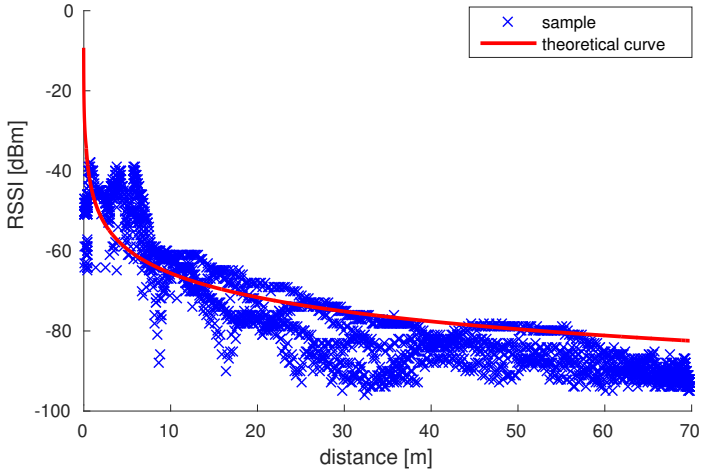

Figure 6.3: Measured RSSI samples depending on a distance with fitted theoretical curve. Antenna on the UAV_2.

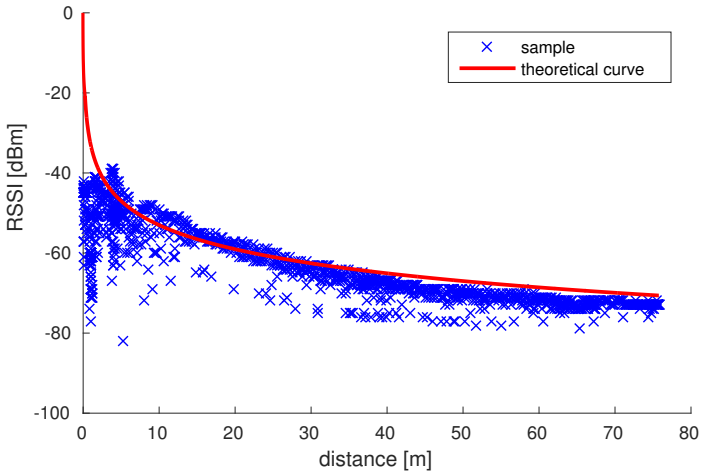

Figure 6.4: Measured RSSI samples depending on a distance with fitted theoretical curve. Antenna on the UAV_3.

Theoretical curves are fitted so that the error (difference between theoretical value and obtained sample) is minimal, mean corresponds to the zero. Therefore, parameters P_0 for each of the antenna are determined as following: $P_{01} = -30.0\text{dBm}$, $P_{02} = -48.5\text{dBm}$, $P_{03} = -33.0\text{dBm}$, where parameters correspond to the antennas on the UAVs respectively.

Unfortunately, the results are unsatisfying. Especially the received signal via antenna on the UAV_2 does not correspond to the theoretical curve well. Moreover, corresponding (UAV_1, UAV_2, UAV_3) standard deviations are $\sigma_1 = 5.3$, $\sigma_2 = 8.2$, $\sigma_3 = 3.5$.

Estimation of the position of a static transmitter is tested with the measured parameters in an experiment. Beacon is placed on the [0, 0] position. Photos from this experiment can be seen in Figure 6.5. And video from this experiment can be seen at youtube [1]. The formation starts with 20m radius at position [-7.86,-17.3]. During the first sequence, estimated position is [13.27, 18]. After the second iteration, estimated position is [82.37, 144.4]. Which is out of the experiment area. The error of the estimation is about 165m. The RSSI is so disturbed, in an attempt to repeat the experiment that triangulation algorithm is not capable of finding intersections of the circles at all.

[1] `https://youtu.be/PiIT9Ddl0eY`

(a) : Starting position.

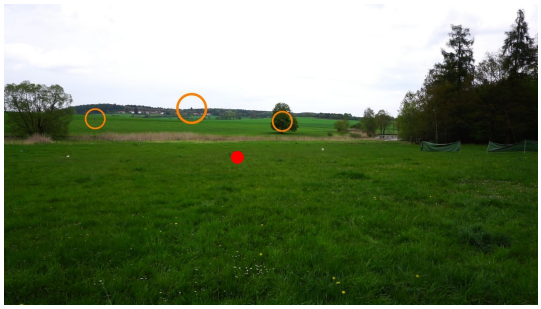

(b) : Position after first reposition.

Figure 6.5: Localization of static beacon with formation of 3 drones.

The characteristics of the receiver antennas are measured again to verify the parameters. Photos from measurement can be seen in Figure 6.6. Video of this measurement can be seen at youtube[2]. For the antenna on the UAV_1 the measured parameters are $P_{01} = -40.8$dBm and $\sigma_1 = 4.6$, for UAV_2 are $P_{02} = -38.9$dBm and $\sigma_2 = 8.2$ and for UAV_3 $P_{03} = -36.7.8$dBm and $\sigma_3 = 10.4$. These parameters differ significantly from the first values. The determination of the parameters of the signal distribution is crucial to determine the distance from the transmitter, because of that, developed algorithm is unable to work due to the instability of the parameters.

In conclusion, as it turns out, the antenna parameters are highly unstable. This is because RSSI is highly influenced by any obstacle. Moreover, reflections and interferences from the UAV change received signal strength significantly. Therefore, it can be stated that XBee platform cannot be considered as a stable and viable option for measuring distance from RSSI.

[2] `https://youtu.be/kDCeoR6pXjk`

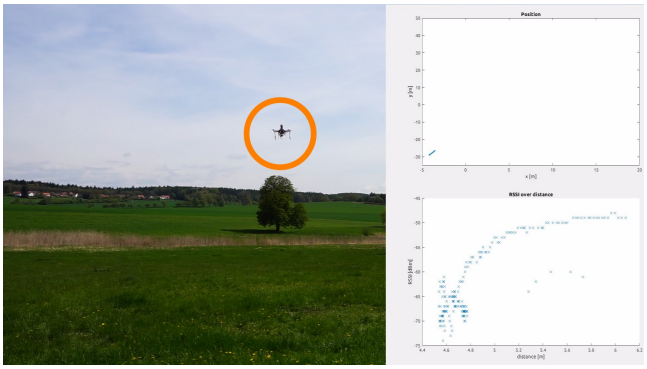

(a) : Time $t = 5$s

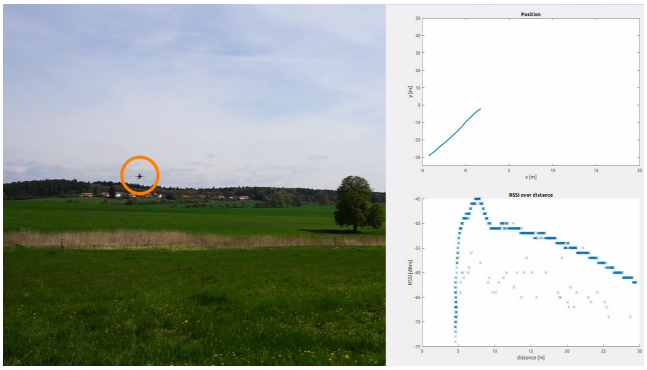

(b) : Time $t = 15$s

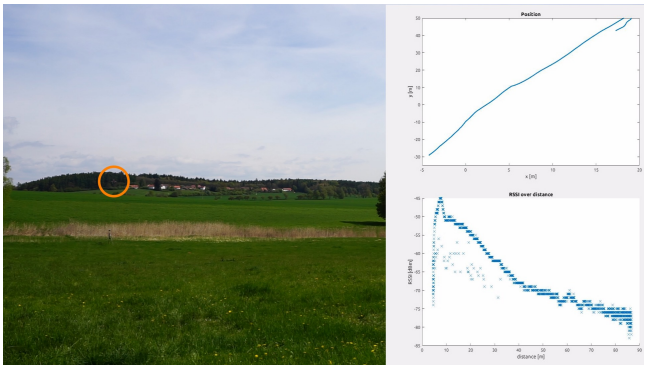

(c) : Time $t = 30$s

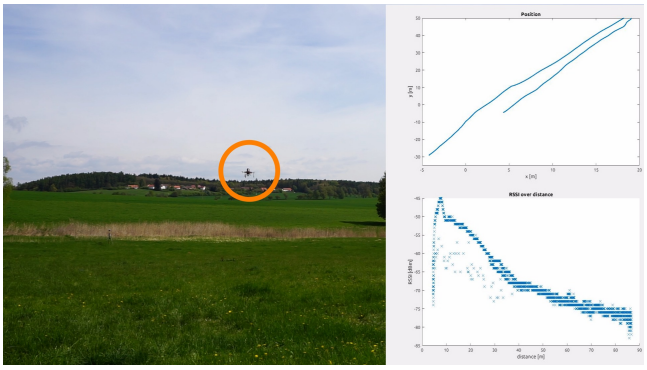

(d) : Time $t = 45$s

Figure 6.6: Measurement of the RSSI characteristic.

Chapter 7

Conclusion

The presented work is a continuation of a long-term research on stabilization and formation flying of UAVs conducted at Multi-robot systems group of CTU in Prague [SVKP14], [SKV+14], [SBS16], [SKP14], [SKV+13], [SVKP12], [SBH16]. The aim of the proposed approaches is to apply of these general methods of formation flying in such a demanding application of real time sensing and consequent RFID localization and to use flexibility of formations (possibility to change their shape and position) to increase precision of localization in a similar way as it was achieved for example in surveillance scenarios [SVC+16], [SBT+16], [SCP+14]. Also here, we rely on unique precise control and motion planning technique based on onboard Model Predictive Control (MPC) [BLS16] of particular MAVs, while the formation stabilization in a compact group is achieved using GPS information and/or mutual visual localization of team members [FKC+13], [KNF+14] in applications in GPS denied environments or in situations, where a small relative distance between UAVs is required (the final phase of the localization process). Although, the mutual localization was not used in the presented experiments (a precise differential GPS was used instead), the method is designed to be able to use it as it was shown in a similar approach in indoor case [Vrb16].

The short summary of this whole thesis is following.

In the Chapter 2.1 a system model is defined with expected parameters of the signal distribution obtained by preliminary measurement. In the whole thesis it is assumed that signal distribution corresponds to the free-space path loss.

The developed system is able to localize beacon in a real time meaning that estimation of position is made during the flight. Therefore, precision of the localization can be improved with active change of the formation. Chapter 3 examines how parameters of the formation affect precision of measurements, and how these conclusions can be used in algorithms. Moreover, the used planar formation is presented in the same Chapter. As the simulation has revealed, the biggest effect on accuracy of the estimation has a relative

position to the formation, the best precision of the estimation is achieved when transmitting beacon is in the middle of the formation.

Two possible scenarios have been expected, localization of the static or moving transmitter, two corresponding algorithms are developed in the Chapter 4. One is the triangulation, and the second one is Unscented Kalman filter. To get the best estimation of the static transmitter combination of both is used in section 4.4.

Tested aproaches are verified in the simulations, which are described in a Chapter 5. As it is shown, precision of the localization of static transmitter is about 0.1m. To localize a moving beacon three approaches have been tested. The first is a triangulation with floating window. As can bee seen in the Figure 5.2, the smallest localization error is when the beacon is in the center of the formation, there, the localization error is 0.85m. Second approach is using UKF with the a-priori knowledge about movement of the beacon. When the a-prior knowledge corresponds to the reality, estimation is better than with the triangulation and it is less conditioned by the relative position of the formation. On the contrary, when the assigned information about movement does not correspond with reality estimation is even worse than with triangulation. The conclusion is, the best method to localize a moving object, if a-prior knowledge exists, is UKF, otherwise, it is better and more robust solution to use triangulation with floating window, and relative position of the formation which center corresponds to the estimation.

To sum up the findings of this thesis, the assumption is that the signal distribution corresponds to the free-space path loss, matching methods are proposed and implemented and they are confirmed in the simulations. The device, which fits this assumption the most, is searched and chosen among available devices being the XBee at the end of this work. In the next step, experimental platform is developed and the set-up is tested with the formation of the three UAV in the real-world conditions. Nevertheless, the use of this concrete device XBee has shown up as less matching the assumption than expected and the search for more fitting device needs to continue. One of the possibilities would be to develop custom antenna with specific parameters, however this option exceeds the limits of this work.

Appendix A

CD contents

The description of the CD directory is written in table A.1.

Directory name	Description
sources	Software source code
thesis	This thesis in pdf format
videos	Videos of experiments

Table A.1: CD Content.

Appendix B

Bibliography

[BLS16] Tomas Baca, Giuseppe Loianno, and Martin Saska, *Embedded model predictive control of unmanned micro aerial vehicles*, Methods and Models in Automation and Robotics (MMAR), 2016 21st International Conference on, IEEE, 2016, pp. 992–997.

[BP00] Paramvir Bahl and Venkata N Padmanabhan, *Radar: An in-building rf-based user location and tracking system*, INFOCOM 2000. Nineteenth Annual Joint Conference of the IEEE Computer and Communications Societies. Proceedings. IEEE, vol. 2, Ieee, 2000, pp. 775–784.

[CDB05] P Cepel, J Duha, and P Brida, *Geometric algorithm for received signal strength based mobile positioning*, Radioengineering (2005).

[CHC06] Yiu-Tong Chan, H Yau Chin Hang, and Pak-chung Ching, *Exact and approximate maximum likelihood localization algorithms*, IEEE Transactions on Vehicular Technology **55** (2006), no. 1, 10–16.

[CK02] Yongguang Chen and Hisashi Kobayashi, *Signal strength based indoor geolocation*, Communications, 2002. ICC 2002. IEEE International Conference on, vol. 1, IEEE, 2002, pp. 436–439.

[FGP+10] Carlo Filoramo, Andrea Gasparri, Federica Pascucci, Attilio Priolo, and Giovanni Ulivi, *A rssi-based technique for inter-distance computation in multi-robot systems*, Control & Automation (MED), 2010 18th Mediterranean Conference on, IEEE, 2010, pp. 957–962.

[FKC+13] Jan Faigl, Tomáš Krajník, Jan Chudoba, Libor Přeučil, and Martin Saska, *Low-cost embedded system for relative localization in robotic swarms*, Robotics and Automation (ICRA), 2013 IEEE International Conference on, IEEE, 2013, pp. 993–998.

[GLBA15] G Greco, Claudio Lucianaz, Silvano Bertoldo, and Marco Allegretti, *Localization of rfid tags for environmental monitoring using uav*, Research and Technologies for Society and Industry Leveraging a better tomorrow (RTSI), 2015 IEEE 1st International Forum on, IEEE, 2015, pp. 480–483.

[Kae06] Kamol Kaemarungsi, *Distribution of wlan received signal strength indication for indoor location determination*, Wireless Pervasive Computing, 2006 1st International Symposium on, IEEE, 2006, pp. 6–pp.

[KCK06] Sang-il Ko, Jong-suk Choi, and Byoung-hoon Kim, *Performance enhancement of indoor mobile localization system using unscented kalman filter*, SICE-ICASE, 2006. International Joint Conference, IEEE, 2006, pp. 1355–1360.

[KNF+14] Tomáš Krajník, Matías Nitsche, Jan Faigl, Petr Vaněk, Martin Saska, Libor Přeučil, Tom Duckett, and Marta Mejail, *A practical multirobot localization system*, Journal of Intelligent & Robotic Systems **76** (2014), no. 3-4, 539–562.

[LL08] Norman HM Li and Hugh HT Liu, *Formation uav flight control using virtual structure and motion synchronization*, American Control Conference, 2008, IEEE, 2008, pp. 1782–1787.

[Mar08] Francesco Martinelli, *Robot localization: comparable performance of ekf and ukf in some interesting indoor settings*, Control and Automation, 2008 16th Mediterranean Conference on, IEEE, 2008, pp. 499–504.

[PDTY09] Daniel J Pack, Pedro DeLima, Gregory J Toussaint, and George York, *Cooperative control of uavs for localization of intermittently emitting mobile targets*, IEEE Transactions on Systems, Man, and Cybernetics, Part B (Cybernetics) **39** (2009), no. 4, 959–970.

[PLM02] Kaveh Pahlavan, Xinrong Li, and Juha-Pekka Makela, *Indoor geolocation science and technology*, IEEE Communications Magazine **40** (2002), no. 2, 112–118.

[PY05] Daniel J Pack and George WP York, *Developing a control architecture for multiple unmanned aerial vehicles to search and localize rf time-varying mobile targets: part i*, Robotics and Automation, 2005. ICRA 2005. Proceedings of the 2005 IEEE International Conference on, IEEE, 2005, pp. 3954–3959.

[QCG+09] Morgan Quigley, Ken Conley, Brian Gerkey, Josh Faust, Tully Foote, Jeremy Leibs, Rob Wheeler, and Andrew Y Ng, *Ros: an open-source robot operating system*, ICRA workshop on open source software, vol. 3, Kobe, 2009, p. 5.

[SBH16] Martin Saska, Tomas Baca, and Daniel Hert, *Formations of unmanned micro aerial vehicles led by migrating virtual leader*, Control, Automation, Robotics and Vision (ICARCV), 2016 14th International Conference on, IEEE, 2016, pp. 1–6.

[SBS16] Vojtech Spurny, Tomas Baca, and Martin Saska, *Complex manoeuvres of heterogeneous mav-ugv formations using a model predictive control*, Methods and Models in Automation and Robotics (MMAR), 2016 21st International Conference on, IEEE, 2016, pp. 998–1003.

[SBT+16] Martin Saska, Tomas Baca, Justin Thomas, Jan Chudoba, Libor Preucil, Tomas Krajnik, Jan Faigl, Giuseppe Loianno, and Vijay Kumar, *System for deployment of groups of unmanned micro aerial vehicles in gps-denied environments using onboard visual relative localization*, Autonomous Robots (2016), 1–26.

[SCP+14] Martin Saska, Jan Chudoba, Libor Precil, Justin Thomas, Giuseppe Loianno, Adam Tresnak, Vojtech Vonasek, and Vijay Kumar, *Autonomous deployment of swarms of micro-aerial vehicles in cooperative surveillance*, Unmanned Aircraft Systems (ICUAS), 2014 International Conference on, IEEE, 2014, pp. 584–595.

[SKP14] Martin Saska, Zdenek Kasl, and Libor Přeucil, *Motion planning and control of formations of micro aerial vehicles*, IFAC Proceedings Volumes **47** (2014), no. 3, 1228–1233.

[SKV+13] Martin Saska, Tomáš Krajník, Vojtěch Vonásek, Petr Vaněk, and Libor Přeučil, *Navigation, localization and stabilization of formations of unmanned aerial and ground vehicles*, Unmanned Aircraft Systems (ICUAS), 2013 International Conference on, IEEE, 2013, pp. 831–840.

[SKV+14] Martin Saska, Tomas Krajnik, Vojtch Vonásek, Zdenk Kasl, Vojtch Spurnỳ, and Libor Preucil, *Fault-tolerant formation driving mechanism designed for heterogeneous mavs-ugvs groups*, Journal of Intelligent & Robotic Systems **73** (2014), no. 1-4, 603.

[SVC+16] Martin Saska, Vojtěch Vonásek, Jan Chudoba, Justin Thomas, Giuseppe Loianno, and Vijay Kumar, *Swarm distribution and deployment for cooperative surveillance by micro-aerial vehicles*, Journal of Intelligent & Robotic Systems **84** (2016), no. 1-4, 469–492.

[SVKP12] Martin Saska, Vojtěch Vonásek, Tomáš Krajník, and Libor Přeučil, *Coordination and navigation of heterogeneous uavs-ugvs teams localized by a hawk-eye approach*, Intelligent Robots and Systems (IROS), 2012 IEEE/RSJ International Conference on, IEEE, 2012, pp. 2166–2171.

[SVKP14] Martin Saska, Vojtěch Vonásek, Tomáš Krajník, and Libor Přeučil, *Coordination and navigation of heterogeneous mav–ugv formations localized by a 'hawk-eye'-like approach under a model predictive control scheme*, The International Journal of Robotics Research **33** (2014), no. 10, 1393–1412.

[Vrb16] Matouš Vrba, *Active searching of rfid chips by a group of relatively stabilized helicopters*, Bachelor thesis (2016).

[WVDM00] Eric A Wan and Rudolph Van Der Merwe, *The unscented kalman filter for nonlinear estimation*, Adaptive Systems for Signal Processing, Communications, and Control Symposium 2000. AS-SPCC. The IEEE 2000, Ieee, 2000, pp. 153–158.

[WYB07] Xiaohua Wang, Vivek Yadav, and SN Balakrishnan, *Cooperative uav formation flying with obstacle/collision avoidance*, IEEE Transactions on control systems technology **15** (2007), no. 4, 672–679.